AN ELECTRONIC ULTRASOUND BACKSCATTER ANALYZER

A Thesis

Presented to

The Faculty of Graduate Studies and Research

The University of Manitoba

In Partial Fulfillment

of the Requirements for the Degree

Master of Science in Electrical Engineering

by

A. W. De Groot

September 1970

ABSTRACT

A portable ultrasound backscatter analyzer is described, which samples and then analyzes, in analog form, the backscattered ultrasound from the object under test. The principal quantities that can be measured with the analyzer are: the average amplitude, the power, and the number of echoes. Also, pulse height analysis can be performed.

The analyzer was developed primarily for the ultrasonic testing of fish tissue, using pulsed ultrasound in the 2 to 7 MHz range. Test points are available which allow signals, that are generated externally, to be fed in and analyzed. The entire instrument, including the transmitter, utilizes solid-state devices - mostly integrated circuits. The transmitter consists of a complementary pair of high-voltage transistors, connected as a silicon controlled rectifier, through which a capacitor is discharged into a transducer. The transducer is used in the transmit/receive mode. Variable gain allows compensation for the absorption in the propagating medium.

The main feature of the analyzer is that the measurement results are displayed on a meter, in contrast to the previously employed technique in which the analysis of the backscatter was obtained from photographs of A-scan oscilloscope traces - a tedious and time consuming task.

Tests performed on samples of fish tissue showed that it is possible to determine, roughly, the temperatures at which the samples had originally been frozen.

ACKNOWLEDGEMENTS

The author expresses his appreciation to Professor G.O.Martens for his guidance throughout this research, and particularly during the preparation of the manuscript.

Sincere thanks are also due to Mr. M.Freese of the Fisheries Research Board of Canada, for many hours of discussion and numerous helpful suggestions.

The financial assistance of the Fisheries Research Board of Canada, and the kind permission to use its laboratory facilities, are also gratefully acknowledged.

TABLE OF CONTENTS

****

TO N.

CHAPTER I

INTRODUCTION

1-1: Basic Principles of Ultrasonic Non-Destructive Testing.

With ultrasonic testing, it is possible to find flaws in materials which are very difficult to detect by other non-destructive methods.

The principles of operation are as follows:
A piezo-electric crystal is excited by a fast-rising pulse, generating short bursts of high-frequency mechanical vibrations. These are transmitted into the object under test. Whenever the sound wave train passes the interface of two different media, or more precisely, two media with different acoustic impedances[1], so that an impedance mismatch exists, a certain fraction (depending on the amount of mismatch) of the acoustic energy will be reflected. This backscattered signal subsequently excites the crystal, which converts these mechanical vibrations into an electrical pulse which may, after amplification, be displayed on an oscilloscope. This is the so-called A-scan presentation. If the oscilloscope is triggered by the transmitted pulse, then the location of the echoes on the cathode ray tube depends on the time of travel from the transducer and back, and hence, if the propagation velocities in the media are known, the locations where the echoes are generated (often referred to as scattering-centres) can be determined.

In practical test set-ups, either of two modes of operation may be employed:

a) the contact-method, where the transducer is held against the sample, and

---

[1] Equal to the square root of the product of compressibility and density.

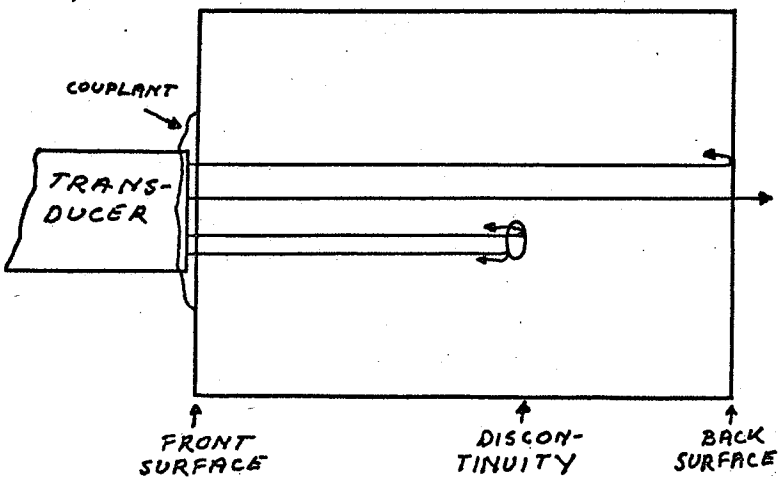

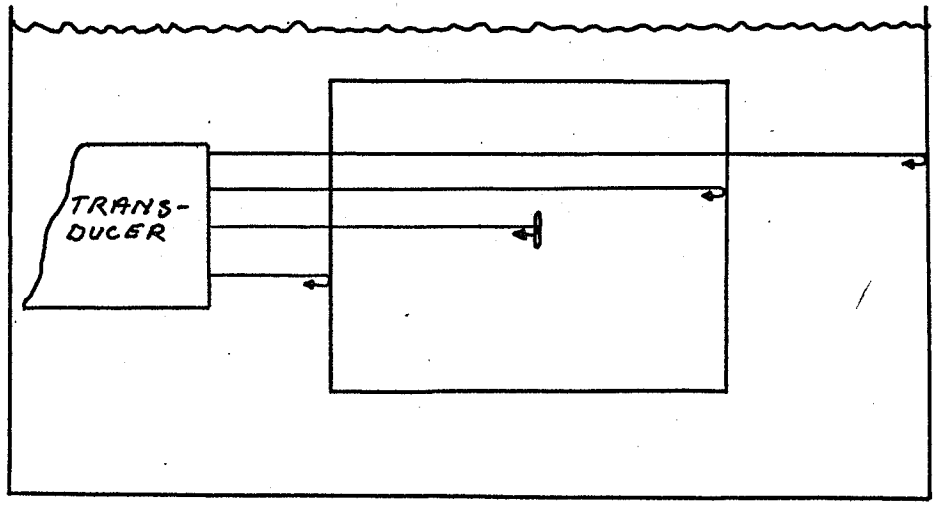

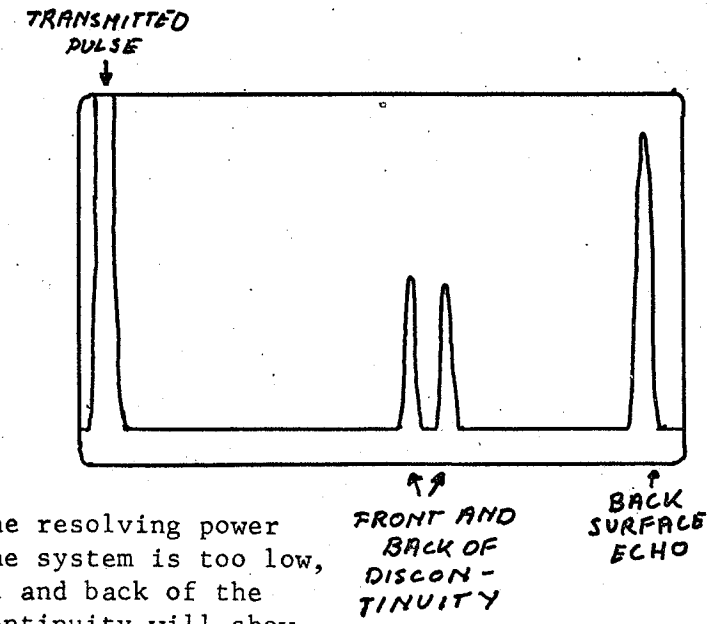

If the resolving power of the system is too low, front and back of the discontinuity will show up as one echo as in Fig.1-1·2.

Fig. 1-1·1.

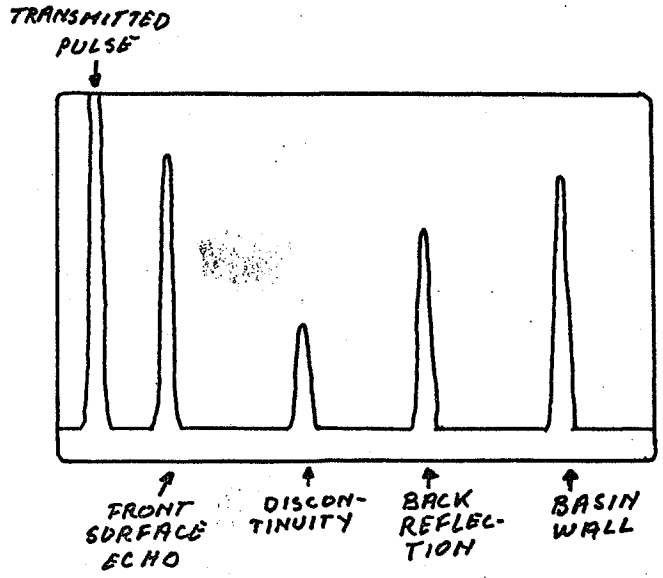

Fig. 1-1·2.

b) the immersion-method, where both transducer and test piece are immersed in a liquid (usually water), with the transducer positioned at some distance from the sample.

When the contact-method is used, proper acoustic coupling is provided by applying an acoustic couplant at the interface of transducer and sample. Figures 1-1·1 and 1-1·2 give an illustration of the principles outlined above.

Although there are several factors involved, it is obvious that the resolving power, which is the ability of the system to distinguish between two sequential echoes whose reflectors lie at different distances on the axis of the sound field, depends on the duration of the transmitted pulse: the shorter the pulse, the greater the resolution. This is the reason why a lithium-sulphate transducer, having a low Q, is employed in the ultrasound analyzer.

1-2: The Application of Ultrasound in the Quality Determination of Fish Tissue.

Experiments determining the ultrasonic properties of fish tissue and the ultrasound back-scatter in fresh and thawed animal tissue were carried out by Freese and Makov [1,2], and some of the important results are discussed in this chapter.

The quality of fish tissue encompasses several factors of differing importance. Some of these factors are: the external appearance of the fish flesh, its texture, odour, taste and freshness· Another factor is freezing. Although freezing may have little effect on the freshness of the flesh, the texture and storage potential may suffer considerably.

It has been found that the backscatter of high-frequency ultrasound from fish tissue differs markedly for fresh tissue and for tissue which has

been frozen and then thawed. Tests have shown that the backscatter is highly dependent on the rate of freezing and the number of times a sample has been thawed and refrozen.

The changes in backscatter are primarily due to the presence of numerous small cavities (scattering-centres) in the tissue, caused by formation of ice crystals and dissolved air which comes out of solution during the freezing process.

The size and number (or rather the spatial distribution) of these cavities, and thus the amplitude distribution of the backscattered signal, depend on the rate of freezing.

For initial measurements, a pulsed transducer ringing at 3.16 MHz for 1.5μsec was used. The ultrasonic beam was directed through a water path at the immersed sample.

A part of the incident beam penetrates the sample and is scattered at tissue interfaces having different acoustic impedances. Some of the scattered energy is reflected back to the transmitting transducer which also serves as the receiver. The received echoes are then amplified, demodulated, and displayed as a function of time, time being approximately proportional to tissue depth.

The type of oscilloscope traces obtained (A-scans) are shown in Fig. 1-2·1 for a sample of fresh and thawed fillet of Whitefish (Coregonus Clupeaformis). The fresh sample, Fig. 1-2·1(a), was scanned and then frozen

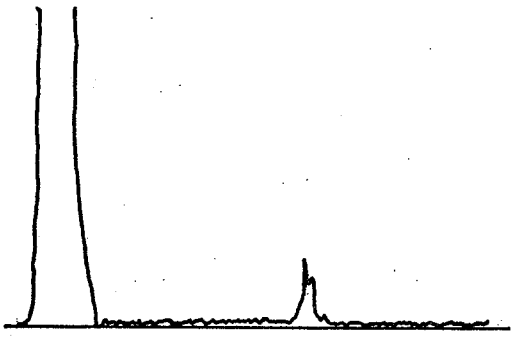

Fig. 1-2·1(a)

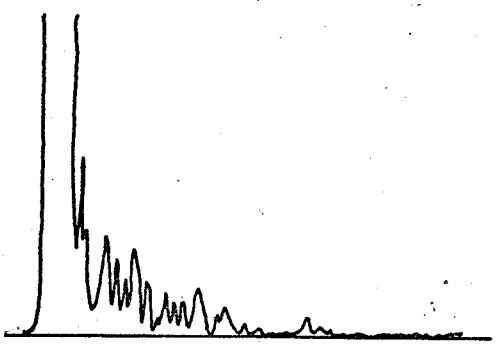

Fig. 1-2·1(b)

at -10^{o}C. After thawing at room temperature, it was scanned again; this A-scan is shown in Fig. 1-2·1(b).

The large pulse at the left of each scan in Fig. 1-2 is the echo from the scales of the fish. The last echo at the right is from the midline of the fish. A great increase in number and amplitude of the echoes between the scale and midline is evident in Fig. 1-2·1(b). The mean amplitudes of these echoes are approximately 16 dB higher than those of the corresponding echoes in Fig. 1-2·1(a).

The number of observable distinct echoes per centimeter of tissue depth (at a particular gain and frequency) is also significant. For example, a moderate freezing temperature (-20^{o}C) results in numerous peaks similar to those in Fig. 1-2·1(b) but having considerably lower average amplitude; a higher freezing temperature (-5^{o}C) results in slightly fewer peaks, but larger average amplitudes.

The original freezing temperature can thus be roughly estimated from the number and amplitude of the echoes.

It should be noted that a sample must always be thawed before a test can be performed.

The exponential decay of the echo amplitudes (only observable in Fig. 1-2·1(b)) is the result of attenuation of the incident and the scattered pulses. The attenuation for fresh and thawed tissue was measured to be 2.3 dB/cm and 4.8 dB/cm (at 3.16 MHz) respectively [2]. These figures increase, however, with increasing frequencies. Similar results were obtained using the contact method.

1-3: Problem Statement

The above observations yield the motivation for the development of an instrument that is capable of determining the freezing history of a sample

of fish tissue through measurement of the number of echoes and/or the average amplitude of the backscattered signal. Measurement results should be available instantly so that a large number of samples may be checked in a minimum amount of time.

CHAPTER II

BASIC REQUIREMENTS OF THE TEST INSTRUMENT AND FUNCTIONAL BLOCK DIAGRAM

2-1: Basic Requirements.

The most important feature of the instrument is that the result of each measurement should appear as an indication on a simple meter. This, of course, rules out the representation of the reflected waveforms as a function of time or distance (such as e.g. the A-scan presentation). Instead we observe the integral effect of the signal in a certain recurring time-interval. To accomplish this, it is necessary to sample a particular portion of desired width and position on the repetitive time axis. Sampling is performed by a gating circuit: when a pulse of sufficient positive amplitude is applied to the gate, it will pass the input signal (with a gain of approximately 20 dB); when the gate pulse is low, it will attenuate approximately 60 dB.

Now suppose transmission is started at a time t_o. Then the positive envelope of the backscattered signal from a fish might look as shown in Fig. 2-1·1.

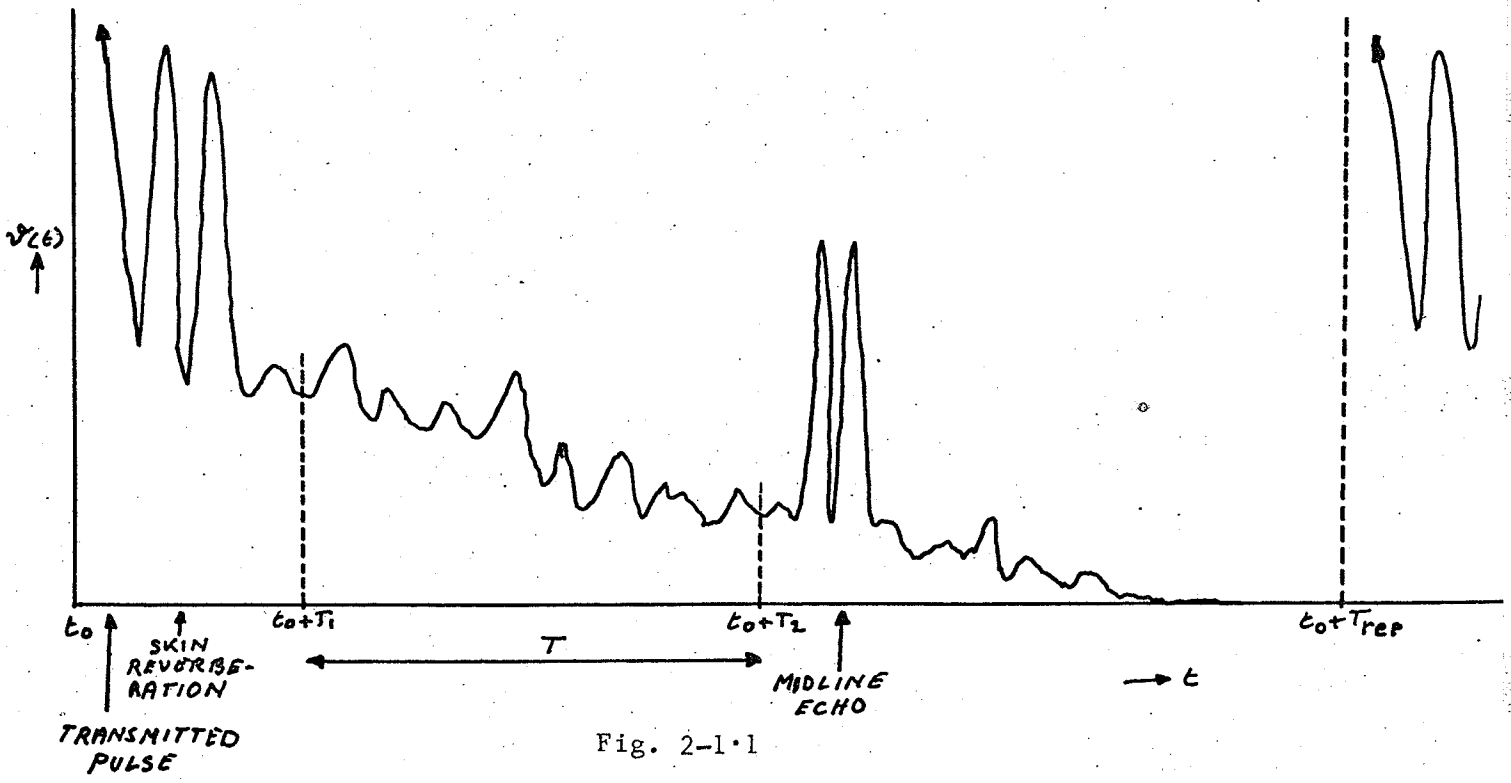

Fig. 2-1·1

The sampled interval has a duration T (from $t_o + T_1$ to $t_o + T_2$). Both T_1 and T_2 are variable. The interval T should, however, not cover the midline echo or the backscatter from the scales, as these signals contain no information relevant to the freezing history of the flesh.

The signal to be analyzed is designated $v_T(t)$, and its square is $v_T^2(t)$;

$$v_T(t) = \begin{cases} v(t) & t_o + T_1 < t < t_o + T_2 \\ 0 & t < t_o + T_1 \text{ and } t > t_o + T_2 \end{cases}$$

These signals are shown in Fig. 2-1·2 and Fig. 2-1·3, respectively.

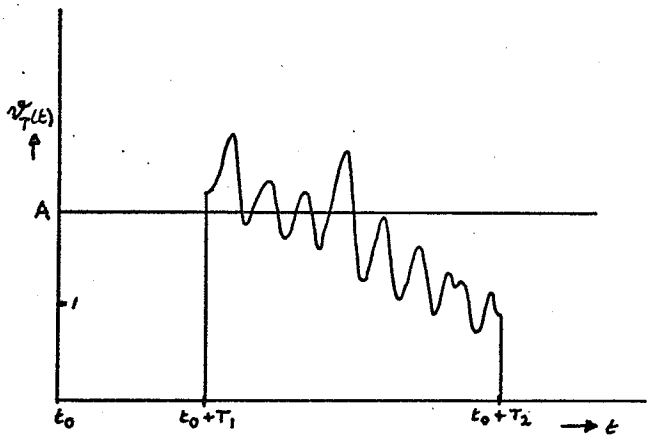

Fig. 2-1·2

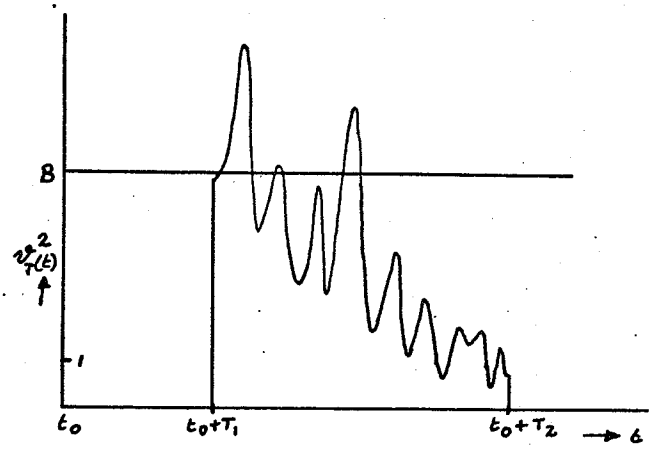

Fig. 2-1·3

The instrument must perform the following measurements:

a) Count the number of echoes, in the interval T_1 to T_2, whose amplitude exceed a certain (adjustable) level A. (In Fig. 2-1·2 there are four such echoes.)

b) Count the number of echoes, in the interval T_1 to T_2, whose instantaneous power exceeds a certain (adjustable) level B. In Fig. 2-1·3 three echoes would be indicated.

We will refer to the adjustable levels A and B as the threshold levels.

c) Integrate the portion of the signal that exceeds the threshold level over the time-interval $t_o + T_1$ to $t_o + T_2$, that is, evaluate:

$$\int_{t_o+T_1}^{t_o+T_2} v_T(t) - A \;\; U_{(v_T(t) - A)} \; dt \qquad \text{(see Fig. 2-1·2)}$$

This amounts to determining the average signal amplitude above the threshold level.

d) Integrate the portion of the square of the signal that exceeds the threshold level, over the time-interval $t_o + T_1$ to $t_o + T_2$, that is, evaluate:

$$\int_{t_o+T_1}^{t_o+T_2} v_T^2(t) - B \;\; U_{(v_T^2(t) - B)} \; dt \qquad \text{(see Fig. 2-1·3)}$$

This means that we measure the average power above the threshold level.

It is clear from the above that if we make the "window" so narrow that the amplitude of the signal does not change appreciably within the window, then the average amplitude measured is proportional to the amplitude at $t = t_o + T_1$. We can then scan the envelope by varying T_1.

Another important feature that the analyzer should have is the ability to compensate for the absorption losses, which means that variable gain has to be introduced.

The requirements described in this section lead to the functional block diagram shown in Fig. 2-1·4.

2-2: Description of the Implementation.

The functional block diagram (Fig. 2-1·4) is implemented in the

[1] U denotes the Heaviside unit step function: $U(x) = \begin{cases} 1 & x > 0 \\ 0 & x < 0 \end{cases}$

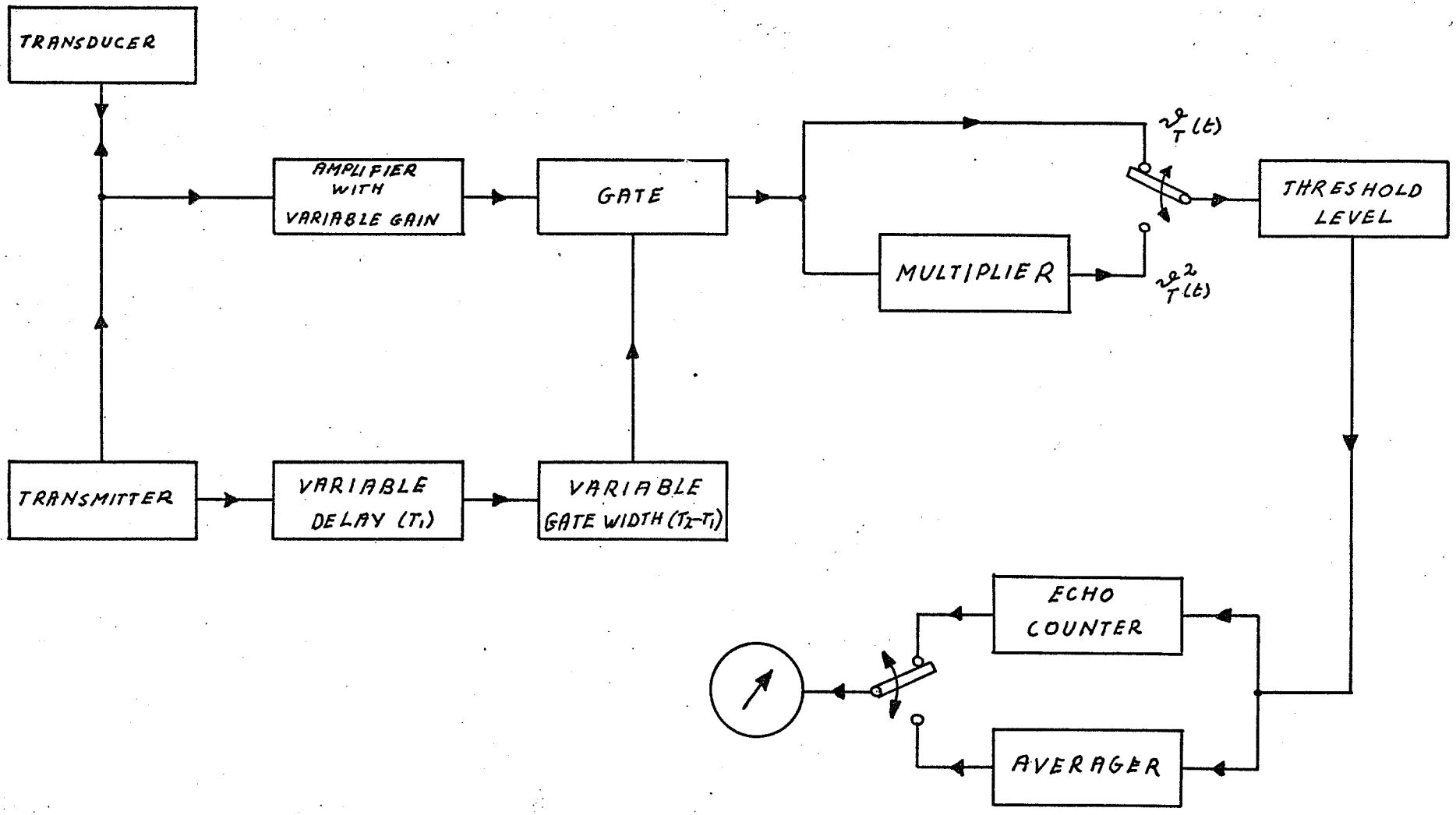

FIG. 2-1-4: FUNCTIONAL BLOCK DIAGRAM OF THE ANALYZER.

detailed block diagram Fig. 2-2·1 on page 12.

As every block will be discussed in detail in Chapter III, we will only give a concise description of the principles of operation in this chapter.

Basically, the analyzer responds to recurring phenomena which have a repetition cycle of T_{rep} seconds. In order to establish a convenient time-scale, we will refer to the times at which each cycle starts ($t_o + n \times T_{rep}$, see Fig. 2-1·1) as t = o, unless otherwise stated.

At t = o the trigger oscillator activates the pulser (a two-transistor switch) which excites the transducer. The coupling network provides proper tuning and damping. The input of the low-noise pre-amplifier (16 dB voltage gain) is preceded by an isolating circuit (limiter) which protects it from the large signals generated by the pulser. The gain of the following pre-amplifier stage can be varied over a range of approximately 26 dB, by changing the value of the feedback resistance. The choice of gain setting will depend upon the level of the backscatter.

In order to offset the attenuation of the sound waves in the fish tissue, the gain of the next stage can be varied by as much as 30 dB in a time interval of 25μsec.

The time at which the gain begins to increase can be chosen as follows: when switch S_1 is in position CON. (contact) the reference monostable, whose output signal is integrated by an operational amplifier to provide a ramp of variable slope, is triggered at t = o; when the switch is in position IMM (immersion) the gain does not change until the gate is opened.

After 40 dB more gain in the next two stages, the gated signal is demodulated by means of a full-wave rectifier and a low-pass filter.

With the switch S_2 we select either the demodulated and gated signal (X), or its square (X^2) for further processing.

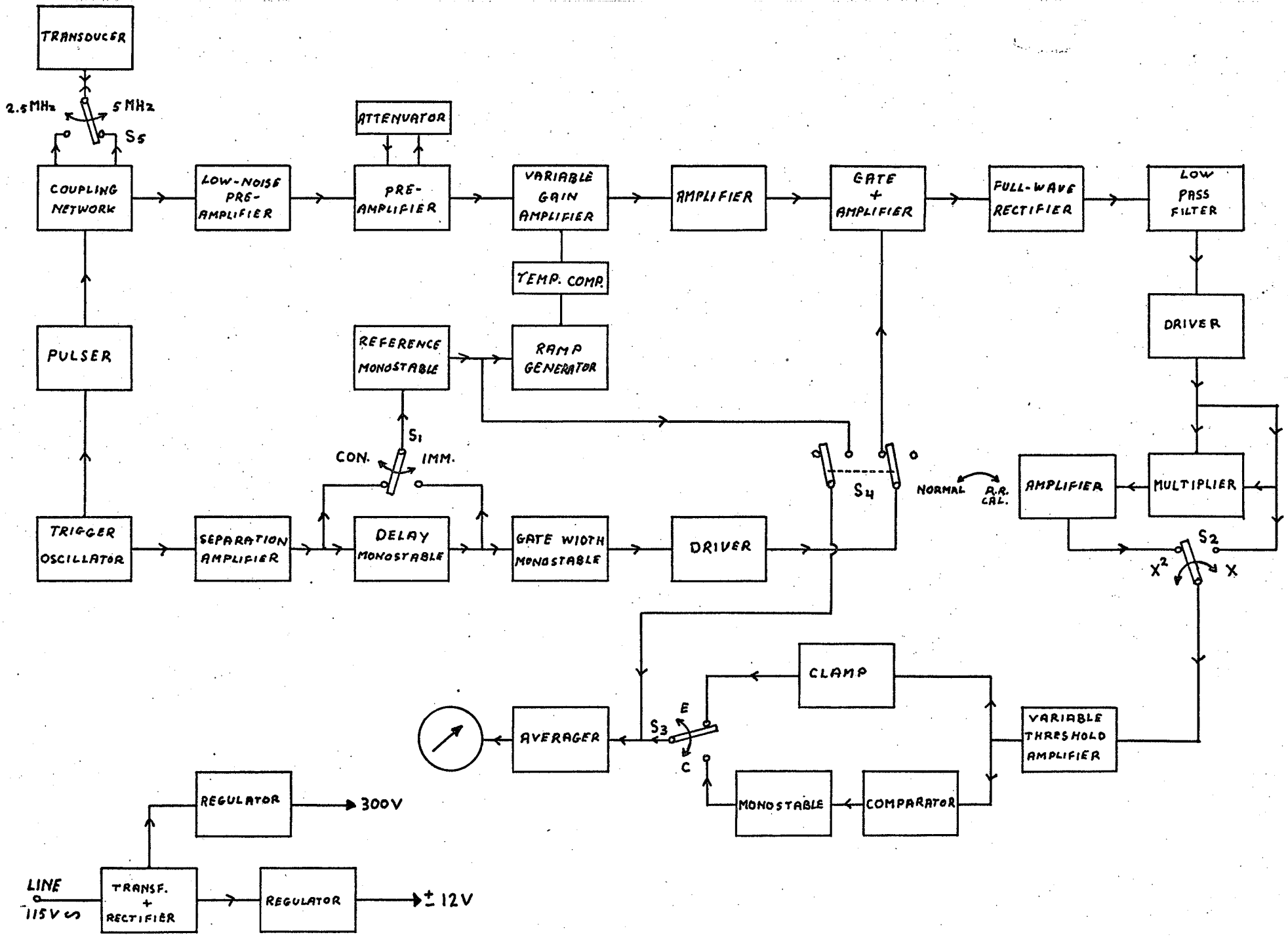

FIG 2-2-1: BLOCK DIAGRAM OF THE ANALYZER

The function of the succeeding stages has been discussed on pages 8 and 9 . When switch S_3 is in position C, the instrument operates in the counting mode, and when it is in position E, integration (or averaging) is performed.

The variable-delay monostable is triggered at t = o. When it returns to its stable state, it triggers the variable gate-width monostable. As long as this mono is in the "high" state, the gate circuit passes the signals. Figures 2-2·2, 2-2·3 and 2-2·4 give an illustration of the various signals.

The target is a 1/8" diameter steel ballbearing immersed in water. The 5 MHz, ½" diameter transducer is located at approximately 1 cm above the ballbearing (Fig. 2-2·5)

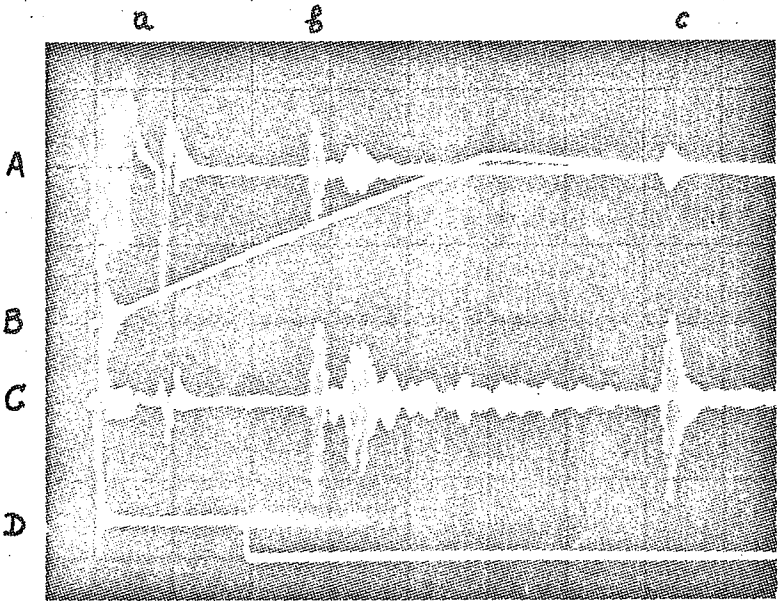

Fig. 2-2·2

Trace A: Backscattered signal $v_{(t)}$ from ballbearing. a is the transmitted signal, b is the echo from the ballbearing and c is the echo from the bottom of the beaker.

Trace B: Ramp which controls the variable-gain amplifier. (S1 in position CON), 200 mV/div, level at beginning of trace: 515 mV.

Trace C: Output of the variable-gain stage.

Trace D: Output of the delay monostable.

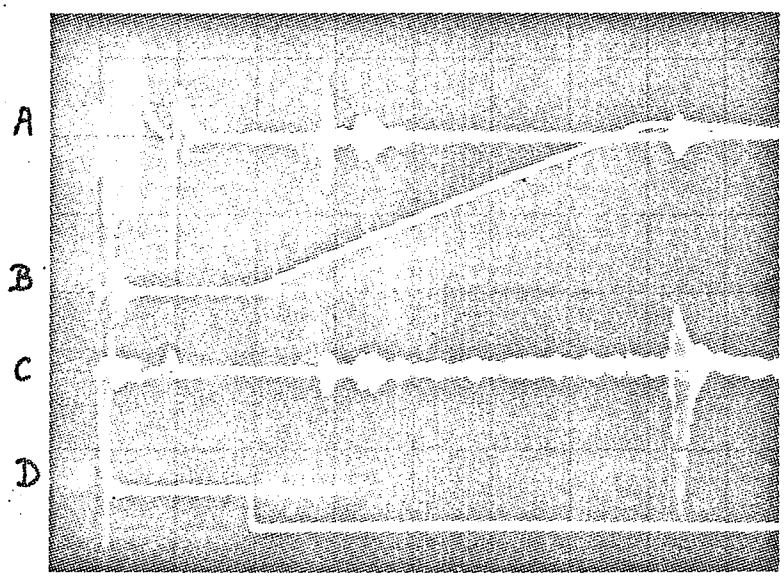

FIG. 2-2·3

The only difference with Fig. 2-2·2 is that S1 is in position IMM.

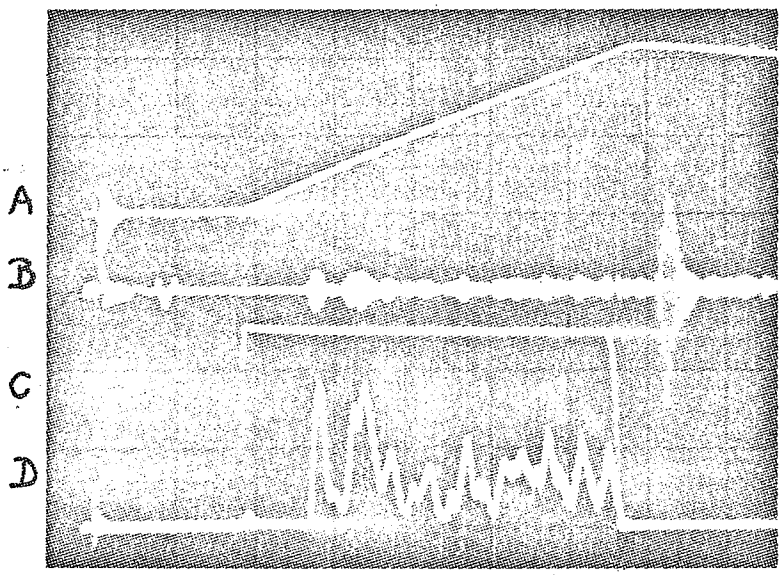

Fig. 2-2·4

Traces A and B correspond to traces B and C, respectively of Fig. 2-2·3.

Trace C: Pulse applied to the gate.

Trace D: Output signal of the low-pass filter.

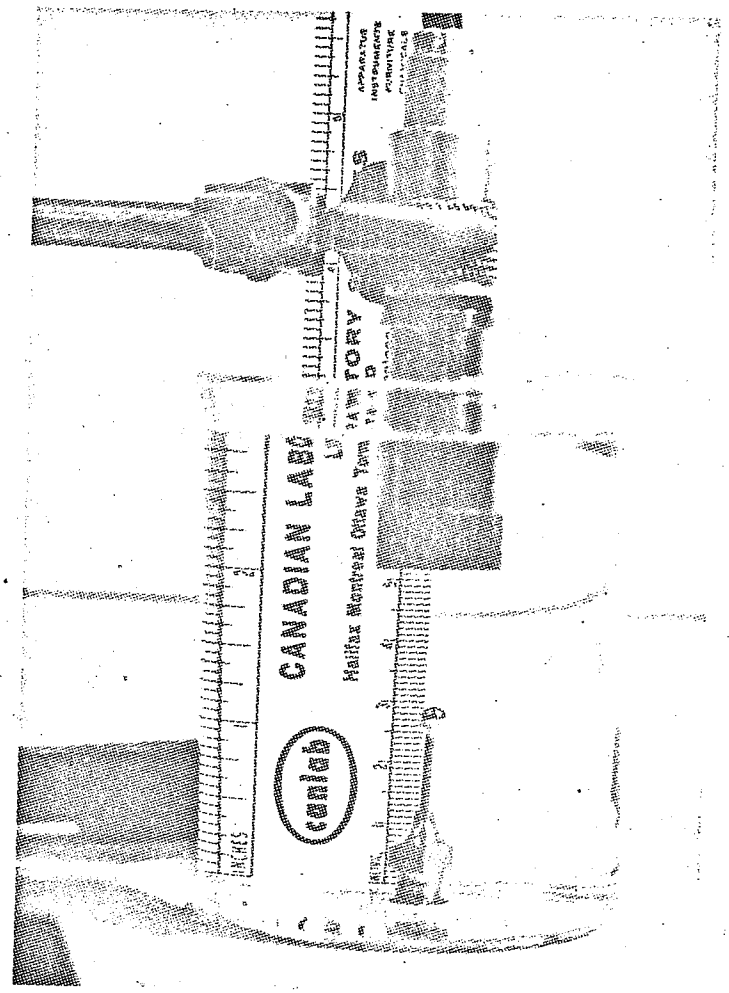

Fig. 2-2·5: BALLBEARING AND TRANSDUCER IMMERSED IN WATER

The repetition rate (frequency of the trigger oscillator) is variable from about 400 Hz to 1100 Hz. An increased repetition rate enhances the accuracy of the measurements. However, the maximum allowable repetition rate is limited by the amount of reverberation, i.e. all echoes generated during a particular cycle must have died out before the next cycle begins, to avoid overlapping of unrelated signals. The amount of "relaxation time" required depends on the absorption coefficients and geometry of the propagation media involved.

Since the measurement results are directly proportional to the repetition frequency, it is necessary to determine this frequency accurately. The repetition frequency can be indicated on the meter by feeding the pulses that are used to generate the ramp for the variable-gain amplifier into the averager. At the same time,the gate is closed, preventing all other signals from entering the averager. The switching is performed by switch S4.

Two regulated power supplies provide 300 volts, required by the pulser, and a balanced ± 12 volts for the remainder of the circuit.

Front - and rear view of the instrument are shown in Figures 2-2·6 and 2-2·7.

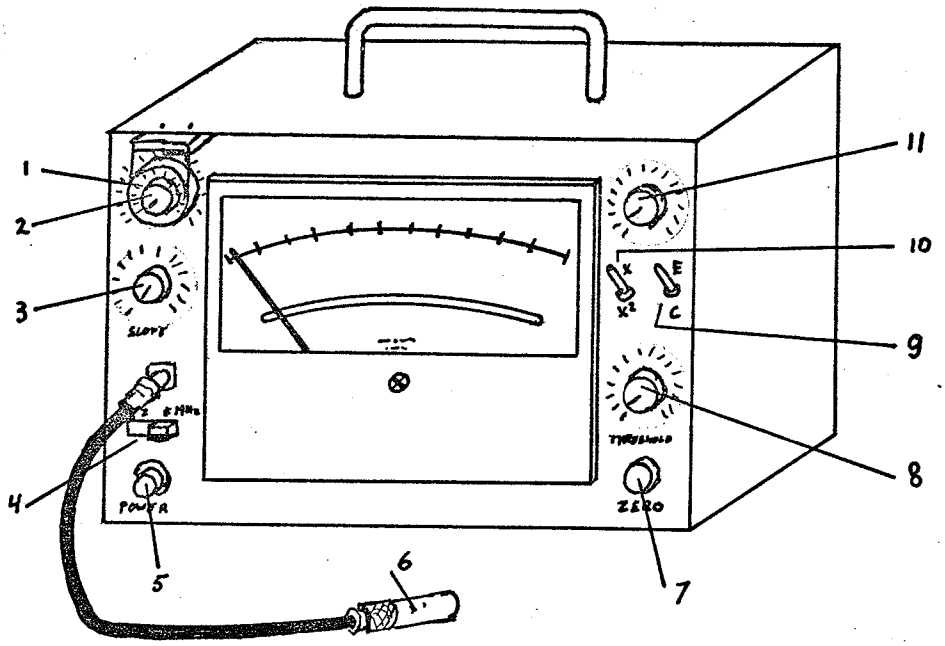

Fig. 2-2·6: FRONT VIEW OF THE INSTRUMENT

1) Gate-width control 2) Delay time control

3) Slope control 4) Frequency selection switch

5) Power switch / pilot light 6) Transducer

7) Zero adjust 8) Threshold level

9) Averaging / counting switch 10) X / X^2 switch

11) Gain control

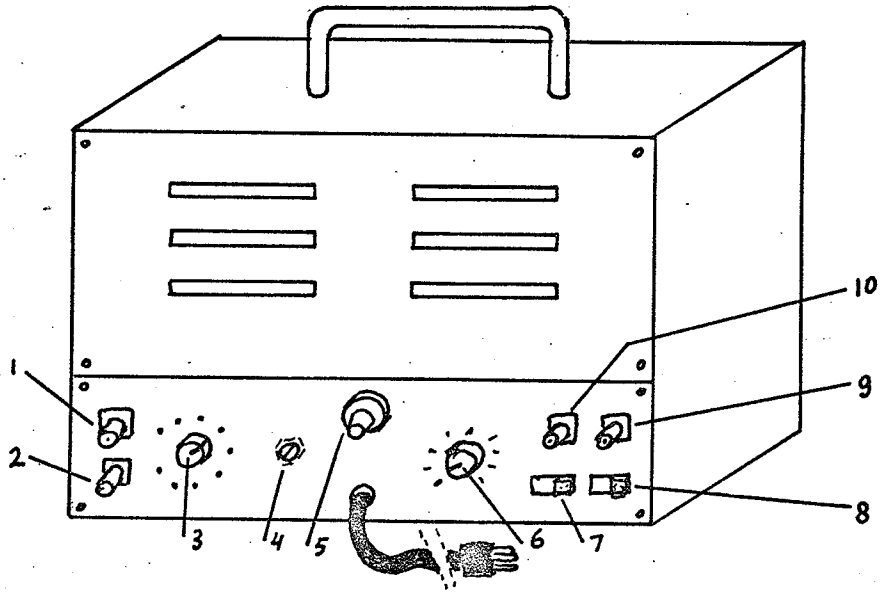

Fig. 2-2·7: REAR VIEW

1) Output pre-amp. 2) Output test-points 3) Test-point selector 4) Gain setting 5) Fuse 6) Repetition rate control 7) Rep. rate calibration switch 8) IMM / CON switch 9) Gate pulse 10) Trigger output

CHAPTER III

CIRCUIT DESCRIPTION AND PERFORMANCE

This chapter is divided into eighteen sections. In each section we discuss a particular block of the block diagram in Fig. 2-2·1, or, whenever appropriate, two or more blocks are discussed simultaneously. The complete circuit diagrams appear in the last section of this chapter.

The complete instrument can roughly be considered as consisting of five major parts. These are:

1) Pulser - and R.F. circuits (sections 1 - 7),
2) Video - and output circuits (sections 8 - 12),
3) Gain control - and timing circuits (sections 13 and 14),
4) Power supply (section 15), and
5) Meter (section 16).

Section 17 covers all topics not discussed in the above sections.

The following designations are used for component values:

A number next to a resistor symbol designates the number of ohms; the letter k, replacing the decimal sign, stands for kilohms (e.g. 1k8 stands for 1800 ohms); and similarly for capacitors, a number beside a capacitor symbol designates the number of picofarads, while 2k2 means 2200 picofarads.

3-1: Trigger Oscillator

The repetition rate of the system is determined by the frequency of the unijunction relaxation oscillator, shown in Fig. 3-1·1.

The frequency of oscillation is determined by R_1, R_2 and C_1, and is (approximately) given by [3]

$$f = \frac{1}{R_T \; C_1 \; \ln \frac{1}{1-\eta}} \quad \text{Hz},$$

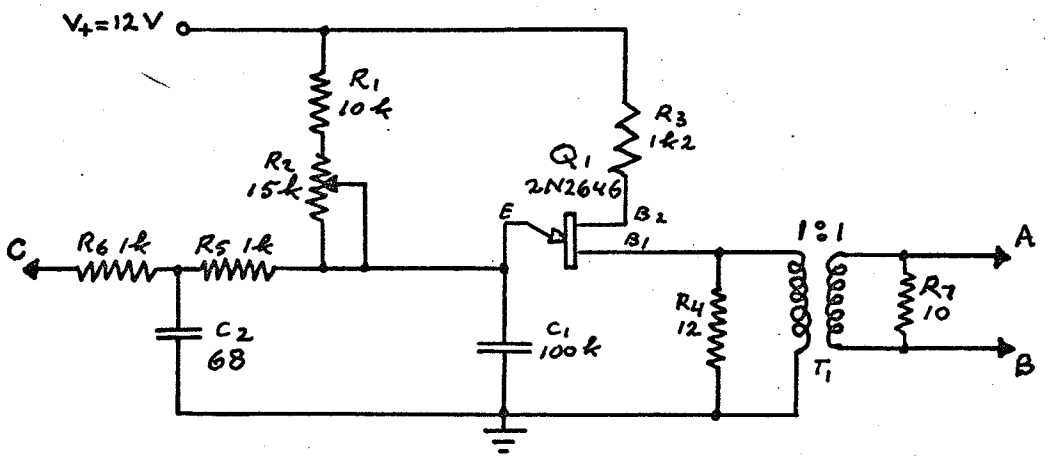

Fig. 3-1·1: TRIGGER OSCILLATOR

where η is the intrinsic stand-off ratio, and R_T equals the sum of R_1 and the active portion of R_2. For the 2N 2646, $\eta \leq 0.65$ and, hence,

$$f \leq \frac{10^7}{R_T} \text{ Hz.}$$

Substituting for R_T 10 kilohms and 25 kilohms, we find for the extreme frequencies 1kHz and 400 Hz, respectively. These values agree well with the measured values of 1100 Hz and 500 Hz, considering that C_1 and R_2 have a tolerance of approximately 20%. Temperature compensation is obtained by making $R_3 = \frac{10000}{\eta\ V+}$. [3]

The pulser (transmitter) is triggered from points A and B. The transformer T_1 is necessary to isolate the transmitter pulse (which is present at points A and B) from ground ; the oscillator circuit resistors R_4 and R_7 provide high damping, which helps the transmitter to turn off quickly. Triggering of the timing circuits is obtained from point C via the low-pass filter consisting of R_5, R_6 and C_2, which prevents the large high-frequency signals, present in the transmitter, from reaching the timing circuits and causing undesired triggering.

3-2: Pulser and Coupling Network

The pulser consists of a two-transistor switch which discharges a capacitor into the coupling network to which the transducer is connected. The cicuit, complete with the transducer equivalent cicuit, is shown in Figure 3-2·1.

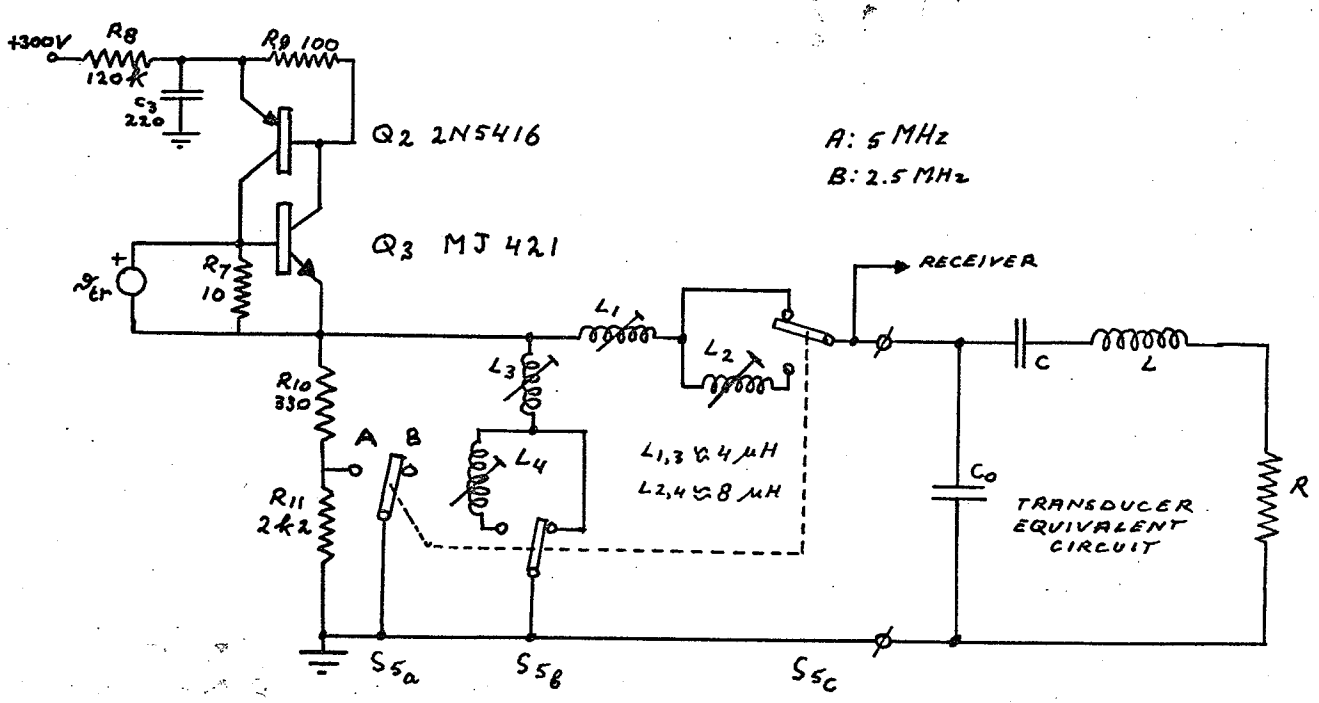

Fig. 3-2·1: PULSER, COUPLING NETWORK AND TRANSDUCER EQUIVALENT CICUIT.

The switch (Q_2,Q_3) is triggered by the oscillator, discussed in the previous section, and represented here by the source v_{tr}. Immediately prior to triggering, capacitor C_3 is charged to 300 volts. When the switch is now turned on, the capacitor discharges, exciting the transducer. Some details regarding the operation of the switch are discussed in Appendix A.

Resistors R_7 and R_9 serve to keep the time during which the switch is ON as small as possible by (a) damping the trigger pulse of transformer T_1 (R_7) and (b) diverting part of the discharge current away from the emitter leads (R_7,R_9). Procedure (a) is especially effective because the switching transients which inevitably appear across the base-emitter junction of Q_3

cause ringing in the pulse transformer which tends to keep the switch ON. At the same time, R_7 decreases the amplitude of the trigger pulse, which decreases its effective width.

Resistors R_{10} and R_{11} provide the necessary damping of the transducer, to obtain echoes of desired duration (approximately 1 μsec). Their values depend on the particular transducers being used and were experimentally chosen.

Tuning to the correct frequency is accomplished by inductors L_1 - L_4, which also control the envelope of the r.f. bursts. The circuit is in fact a rudimentary form of the Ashby line [4]. Figure 3-2·2 shows the voltage across capacitor C_3, starting at time of triggering. It can be seen that the switch remains closed for 5 μ sec.

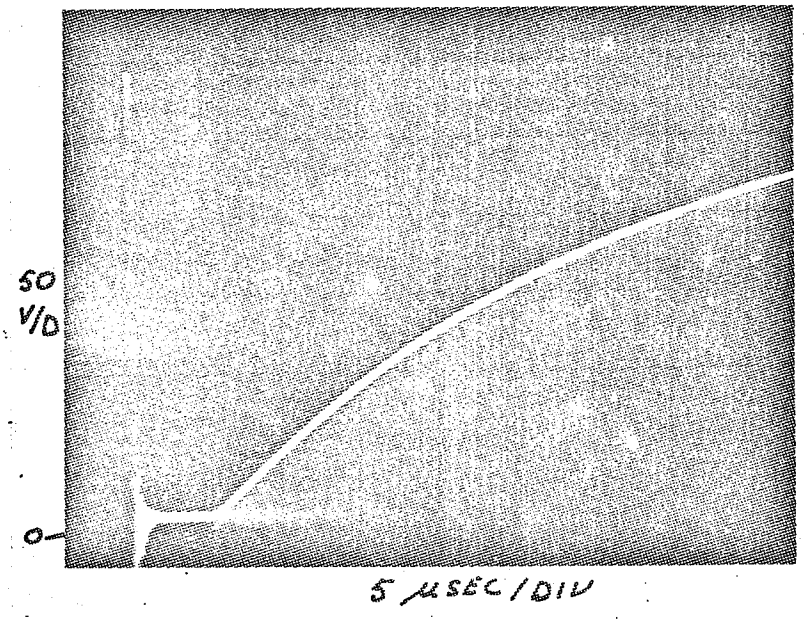

Fig. 3-2·2: CAPACITOR DISCHARGE AND CHARGE CURVE

Figure 3-2·3 shows the r.f. burst, developed across the transducer terminals.

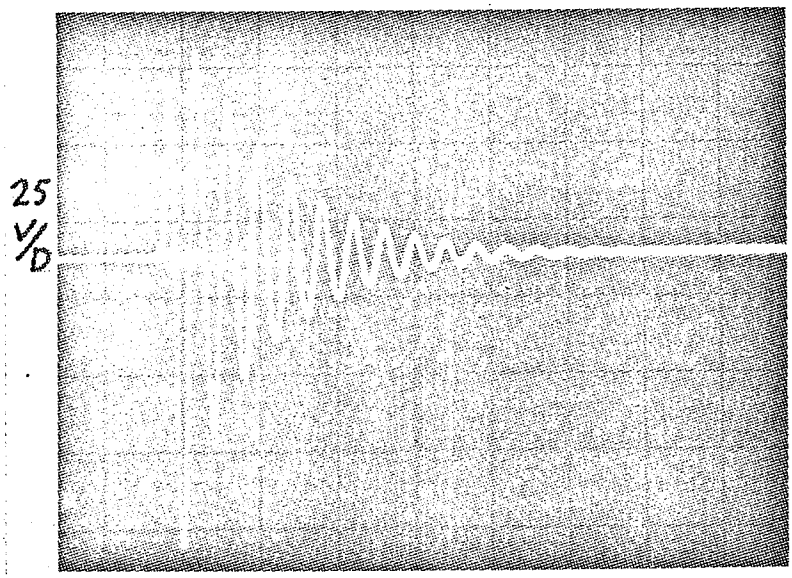

Fig. 3-2·3: R.F. BURST ACROSS THE TRANSDUCER TERMINALS

When the capacitor C_3 was discharged through the switch into a resistive load, the voltage across that load had a risetime of 38 nanoseconds. Experiments with a fast SCR (MC 1336-6) produced negative results at low voltages ($\simeq$ 25V) risetimes in the same range were obtained (34 - 40 $n$sec, depending on the load, which consisted of a capacitor in parallel with a resistor), but at higher voltage levels (250 - 300 v) the risetimes increased to approximately 65 $n$sec, while the required trigger current became prohibitively large (more than 1/4A). Also, the price of both transistors was only one fourth of that of the S.C.R.

3-3: Low Noise Isolating Pre-Amplifier

The input transistor is preceded by a diode limiter, so that it is protected from the large signal (165 V p.t.p.) appearing at the transducer terminals during the transmission cycle. The diodes D_1 and D_2 (see Figure 3-3·1) are high-conductance germanium signal diodes and together with R_{12} and C_4 they form a voltage divider which keeps the signal below 3 volts peak

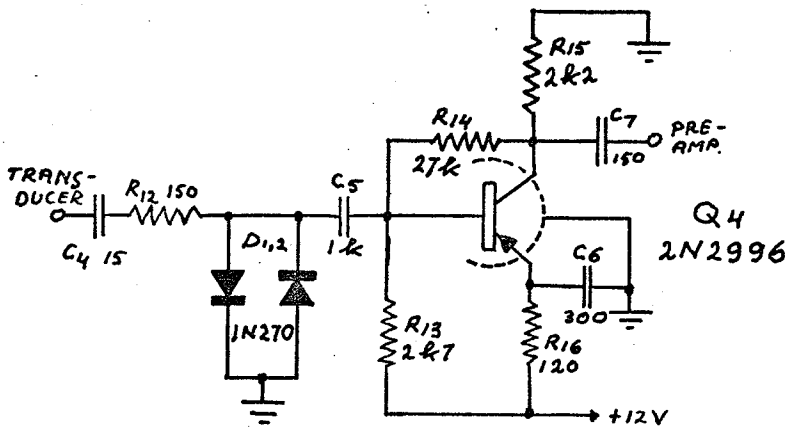

Fig. 3-3·1: LIMITER AND INPUT TRANSISTOR

to peak.

The transistor is a low-noise type (N.F. $< 2\frac{1}{2}$ dB), however, the noise performance of this stage is not too critical, as most of the noise detected at the demodulator is generated in the variable gain amplifier (see section 3-5). The stage has a gain of 16 dB.

3-4: Pre-Amplifier

As a pre-amplifier the RCA CA 3022 was chosen because of its good frequency response (3-dB B.W.: 7.5 MHz) and excellent temperature characteristics ($< \frac{1}{2}$ dB from - 25°C to + 25°C). The circuit is shown in Figure 3-4·1. The gain of the stage is adjustable and is determined by the

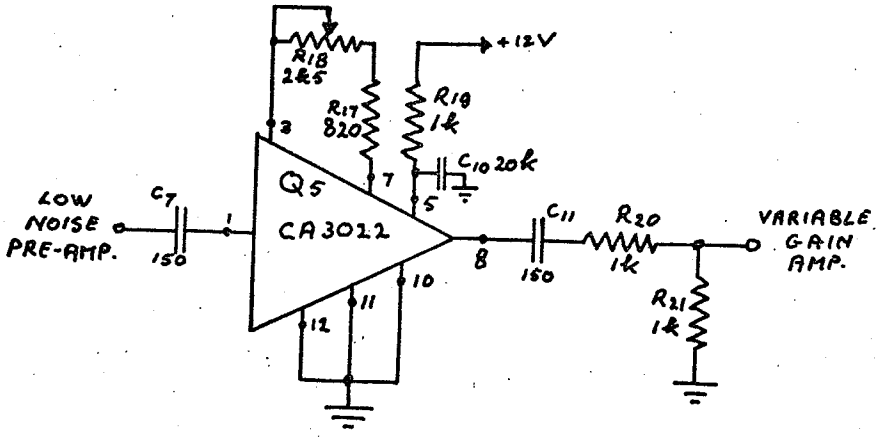

Fig. 3-4·1: PRE-AMPLIFIER

resistance in the feedback loop (R_{17} and R_{18}). R_{17} and R_{18} were chosen such that the gain can be varied between approximately 5 and 31 dB.

As it was necessary to keep the input resistance of the variable-gain stage low (see next section), a series resistance (R_{20}) was included in the output loop to prevent distortion, due to loading, at high signal levels.

The combination R_{19} - C_{10} is the power-supply decoupling network.

3-5: Variable-Gain Amplifier.

The purpose of the variable-gain amplifier is to off-set the attenuation of incident and reflected waves due to absorption in the tissue. Physically, this means "equalization" of the echoes, or introducing dynamic compression. In mathematical terms: the function v(t) (the backscattered signal) is multiplied by a (known) weighting function $v_2(t)$ and, hence, no information is lost. From experimental data [1] we learn that, depending on the freezing history of the tissue, the absorption coefficient at 5 MHz may vary approximately between 0.3 and 0.8 cm^{-1}. Multiplying absorption coefficient and velocity yields the attenuation coefficient which varies between 0.45×10^5 and 1.2×10^5 sec^{-1}, which is equivalent to 0.39 - 1.05 $dB/\mu sec$ (and 2.6 - 7 dB/cm). These figures are lower at lower frequencies. If we want to cover a time-interval of 25 μsec, which corresponds to a tissue depth of 4 cm, we need at most a change of gain of 25 x 1.05 = 26 dB. For the variable-gain amplifier we use a Motorola MC 1545, which is a gate-controlled two-channel-input wideband amplifier. A typical gate characteristic, as published by the manufacturer [5] is shown in Figure 3-5·1. It can be seen that below a certain gate voltage the gain varies exponentially with this voltage, and it is this linear portion of the curve that we use in our application.

The slope of the linear part of the gate characteristic is, according

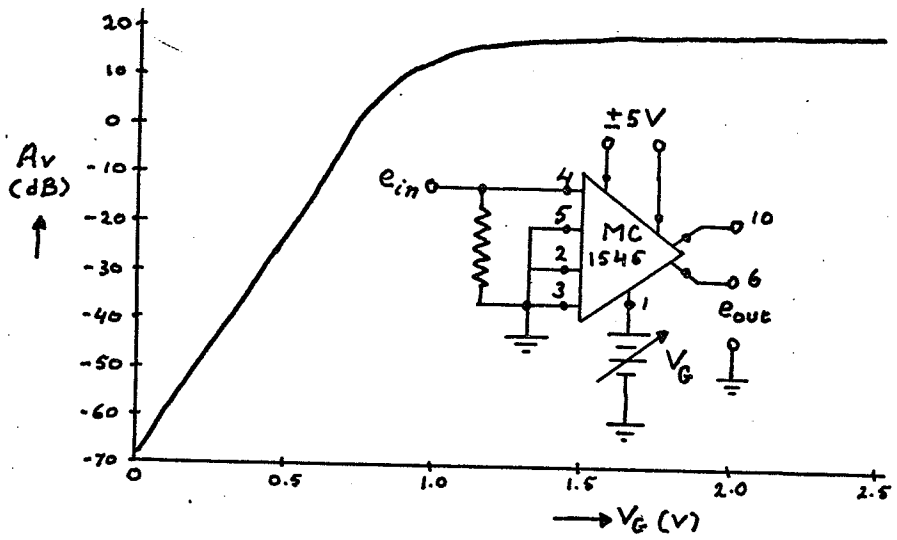

Fig. 3-5·1: GATE CHARACTERISTIC

to Figure 3-5·1, 0,1 dB/mV for a supply voltage of ±5V. Measurements performed on two samples produced different results: 0,08 dB/mV and 0,05 dB/mV.

This means that recalibration will be required whenever the integrated circuit is replaced. Figure 3-5·2 shows how the I.C. is implemented. As the gate is operated in an analog manner and, since the sensitivity of the gain

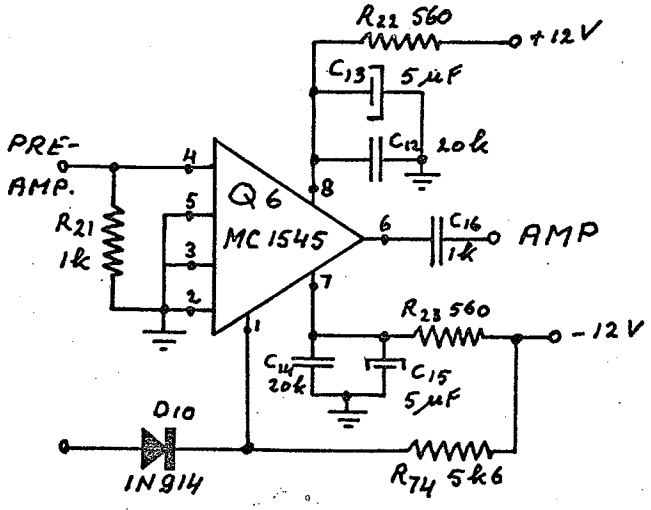

Fig. 3-5·2: VARIABLE-GAIN AMPLIFIER.

to small variations of the gate voltage is relatively high, it is necessary to compensate for the voltage drift, due to changes in temperature, of the internal diode which is connected in series with the gate pin. This is accomplished by using another (silicon) diode with opposite polarity (D 10), so that the temperature drift of the two diodes will, ideally, cancel. Using a 1N914 as a compensating diode gives a temperature coefficient of = 0.2 mV/^{o}C, which is an order of magnitude improvement over the uncompensated gate. R_{74} provides the necessary forward bias of D 10. A ramp voltage (see section 3-13) at the gate produces the desired exponential gain versus time characteristic.

It is evident that the "starting point" on the gain versus gate-voltage curve should be chosen as high as possible for the following reasons:

a) a low point on the curve would cause so much attenuation, that the noise performance becomes very poor;

b) the lower the starting point, the closer the input differential amplifier is biased to cut-off. This may cause serious distortion of the larger input signals.

The purpose of the large capacitors C_{13} and C_{15} is to keep the voltage at the supply terminals (pins 7 and 8) constant when the biasing is being changed by means of the ramp at the gating pin. The equalizing effect of the variable-gain amplifier is shown in Figure 2-2·3 (compare traces A and C).

3-6: Amplifier

The amplifier stage consists of a single transistor in the common-emitter configuration, as shown in Figure 3-6·1.

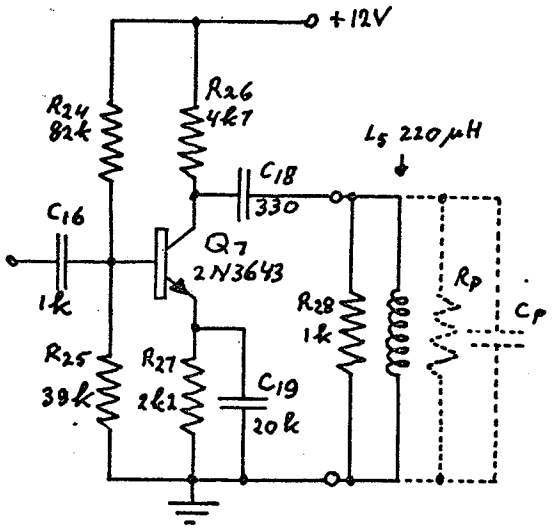

Fig. 3-6·1: COMMON EMITTER AMPLIFIER

The parallel combination of C_p and R_p represents the input impedance of the succeeding stage. Capacitance C_p is constant (6 pF), but the parallel input resistance changes from 10 kΩ at 2MHz to 7 kΩ at 6MHz. However, R_p is in parallel with R28 (1 kΩ) and R26 (4.7 kΩ), and, as a result, the resistive load is quite constant, as capacitor C_{18} also helps to cancel changes in R_p. Inductor L_5 tunes out C_p, but no peaking occurs because the Q is very low (≈ 1/10). The inductor is also used for a different purpose, as will be explained in section 3-7. The gain of the stage is 21 dB.

3-7: Gated Amplifier, Gate-Signal Driver and Full-Wave Rectifier

This part of the system is shown in Fig. 3-7·1. The MC 1445 used here is identical with the MC 1545, except for a limited temperature range (down to 0°C). Any possible dependence of the gate-characteristic upon the temperature is of no consequence, as the amplifier is either completely "ON" (23 dB gain) or completely "OFF". Under normal operating conditions, i.e. the amplifier is gated once every cycle, switch S_{4a} is in position 1. The base of the driver Q_{23} is connected to the output collector of the gate pulse

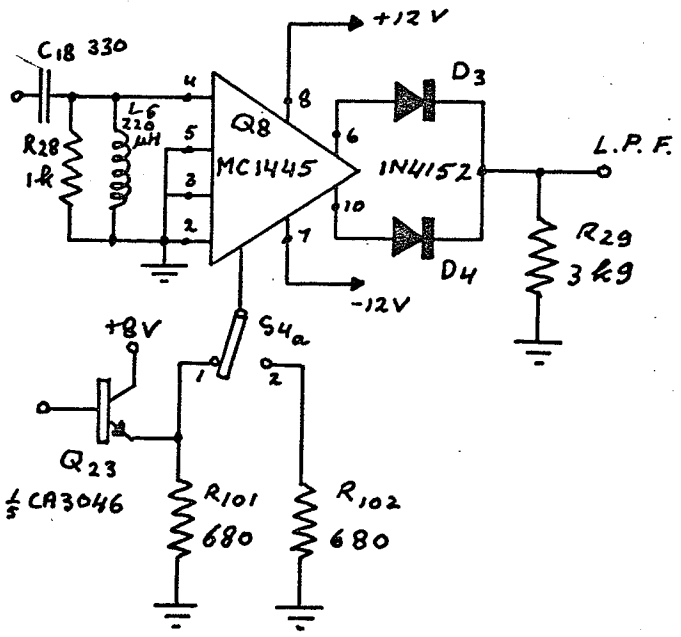

Fig. 3-7·1: GATE AND RECTIFIER CIRCUIT

monostable. When the base of Q_{23} is high, the amplifier is "ON", and the gate (pin 1) draws no current as the internal diode, which is in series with the gate connection, is reverse biased.

When the base of Q_{23} is low, there is no emitter current, but the value of R_{101} should be low enough to allow the gate current required to cut off the amplifier to flow through it. To calibrate the repetition rate of the trigger oscillator, S_{4a} is switched to position 2, which causes the amplifier to be "OFF". For details regarding the repetition rate calibration, refer to section 3-13.

The inductor L_5 prevents the gate-pulse from appearing at the output terminals (6) and (10), by providing a low-resistance path for the amplifier bias current. The amplifier has a differential output stage, making full-wave rectification possible. The quiescent D.C. output level (the voltage at terminals (6) and (10) in absence of an input signal) is about 2.6 volts. The value of R_{29} is chosen such that the quiescent voltage at point A

(Fig. 3-7·1) is approximately 2.1 volts, which causes the silicon signal diodes D_3 and D_4 to be slightly forward biased. Thus, most of the diode off-set is eliminated. The test set-up and the measured result are shown below.

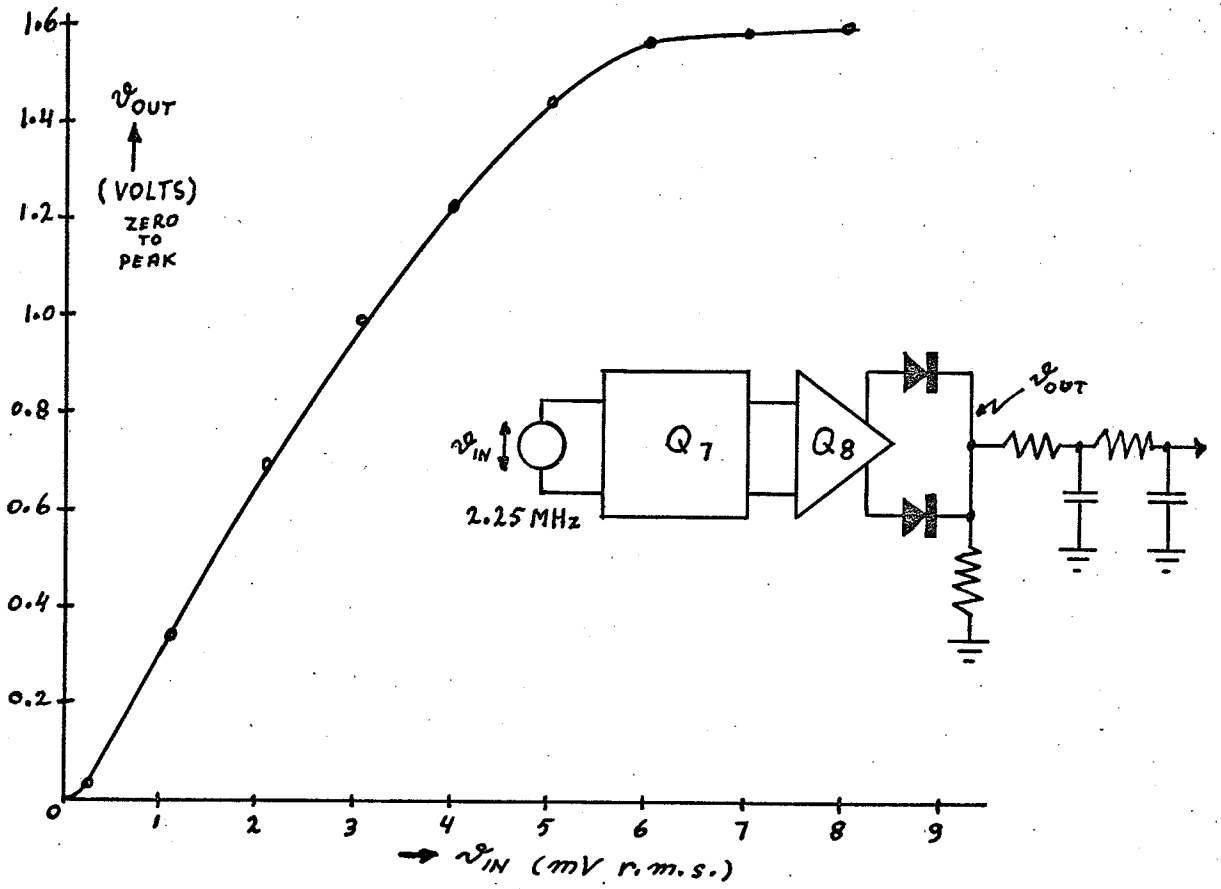

Fig. 3-7·2: RECTIFIER OUTPUT CURVE

Figure 3-7·3 shows the transfer curve of the system, from the input (Q_4) to the differential output of Q_8. The test set-up is also shown.

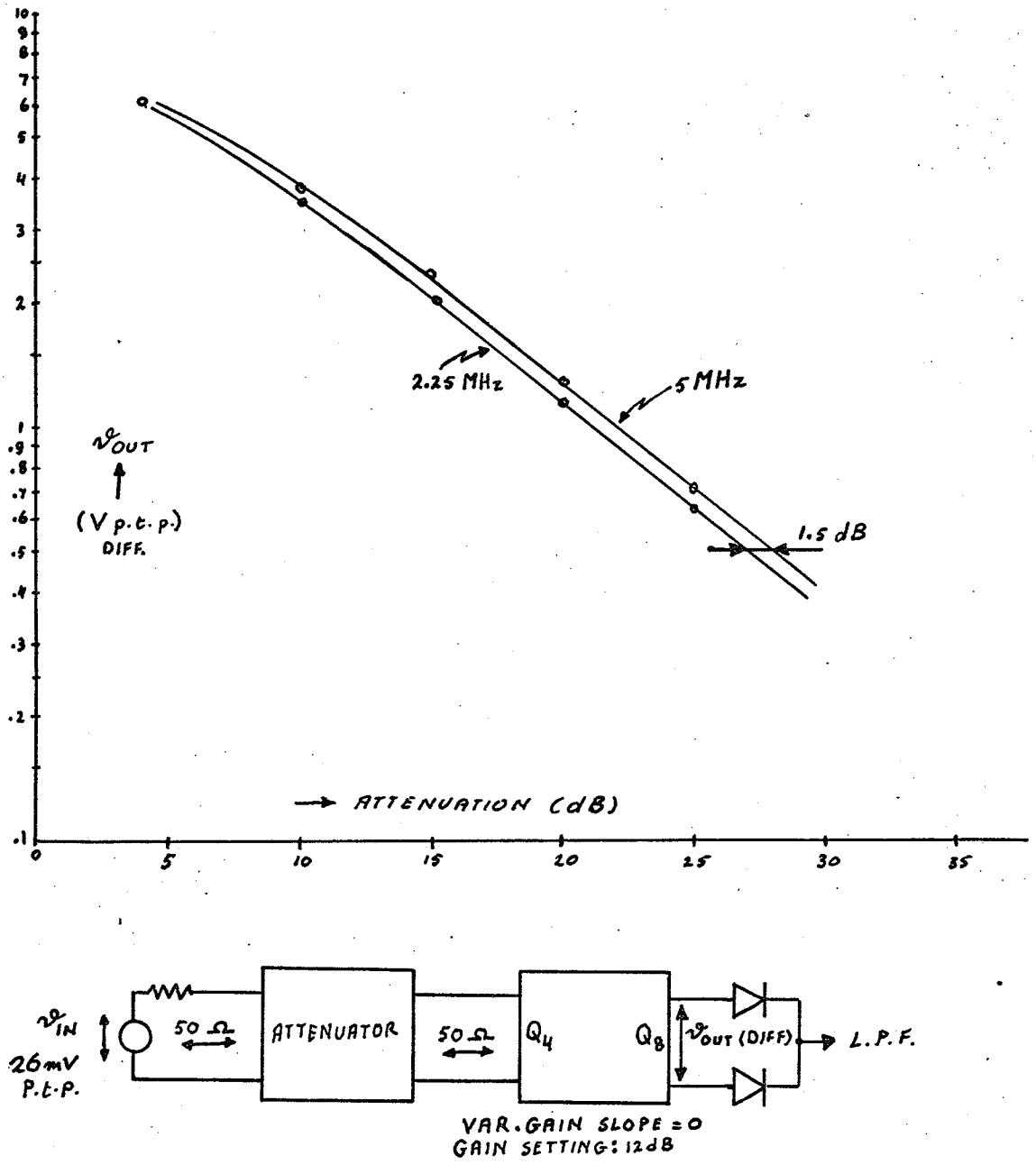

FIG. 3-7-3: TRANSFER CURVE

3-8: Low-Pass Filter and Driver

Experiments have shown that best results are obtained when the echoes have a width of about 1μsec. This is achieved by choosing appropriate values for the damping resistors R_{10} and R_{11}. Therefore, the highest modulation frequency we may expect is approximately one third of the carrier frequency. For the highest carrier frequency used (5MHz) this corresponds to 1.7MHz. Thus, the cut-off frequency of the low-pass filter should be chosen somewhat higher than 1.7MHz.

The actual circuit configuration is shown in Fig. 3-8·1.

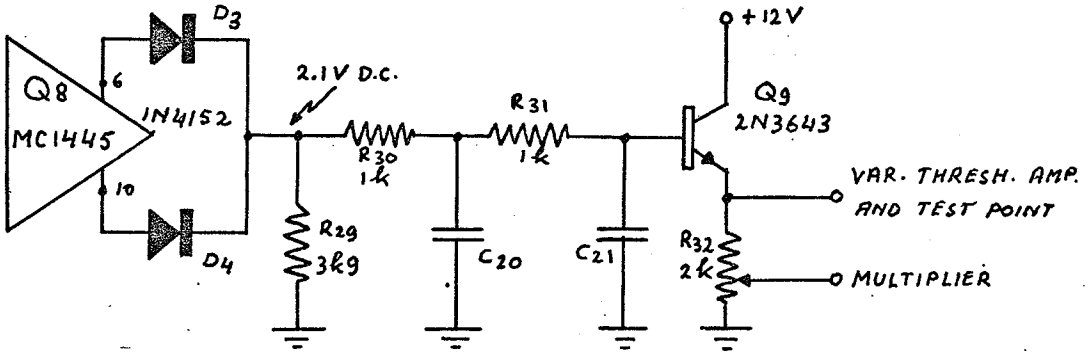

Fig. 3-8·1: RECTIFIER, LOW-PASS FILTER AND DRIVER

The biasing voltage of the driver is obtained from the quiescent D.C. output level of Q_8 through the diodes and R_{30} and R_{31} and is equal to this D.C. level minus the drop across the diodes. The drop across R_{30} and R_{31} is negligible, as the base current of Q_9 is of the order of a few micro-amperes.

As the input impedance of the driver is very high, and the output impedance of the rectifier very low ($\backsimeq$ 30 ohms), we may use the shown equivalent circuit where the low-pass filter is driven from a voltage source and is not terminated. Then the voltage transfer ratio for the filter is given by:

$$\frac{V_3}{V_1} = \frac{1}{(1+ sC_1R_1)\ (1+ sC_2R_2) + s\ C_2R_1}$$

We let $R_1=R_2$ =1kilohm and $C_1= C_2= C$. If we choose a 3-dB-down frequency of 2 MHz, the appropriate value of C can be determined from:

$$\left|\frac{V_3}{V_1}\right|^2 = \left|\frac{1}{(1+ s_oC\ R)\ (1+ s_o\ C\ R) + s_oC\ R}\right|^2 = 1/2,$$

where $s_o = j\omega_o = j\ 2\pi \times 2 \times 10^6$ rad/sec.

Solving the above equation for C yields C = 39 pF.

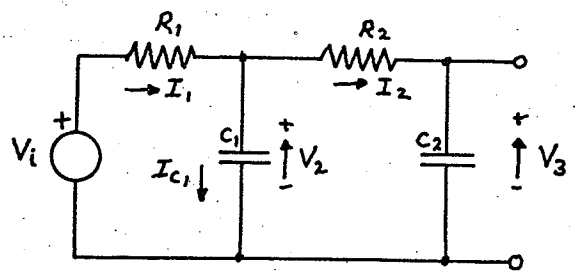

Fig. 3-8·2: LOW PASS FILTER

In practice it was found that the cut-off frequency could be made somewhat lower, as the earlier-mentioned maximum modulation frequency of 1.7 MHz is in fact a little lower. Therefore, the value of C_{21} was increased from 39 pF to 50 pF.

The driver stage features a low output impedance, and its emitter is therefore an ideal testpoint for monitoring purposes.

3-9: Multiplier and Amplifier

As a multiplier we use a Silicon General SG 1402 linear I.C. A simplified schematic diagram of this device is shown in Fig. 3-9·1. The principle of operation is as follows:

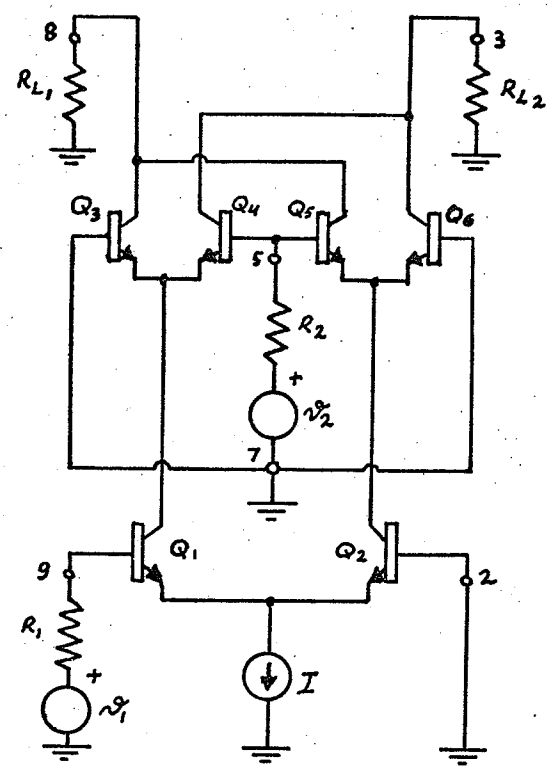

Fig. 3-9·1: SIMPLIFIED SCHEMATIC DIAGRAM OF THE MULTIPLIER

When the voltage source v_1 is equal to zero, the current, delivered by the constant-current source I is divided equally between the differential amplifiers consisting of the transistor pairs Q_3-Q_4 and Q_5-Q_6. The collectors of the transistors are cross-coupled and have common load resistors R_{L1} and R_{L2}. Therefore, independent of how the bias current (I) is distributed between both differential amplifiers, the same current ($\frac{1}{2}$I) flows through both load resistors at all times. As a result, there is no change of potential across R_L when v_1 departs from zero, causing an unbalance in the current distribution. This holds true only when v_2 is equal to zero. A change in the bias current, however, causes a change in the gain of the differential amplifiers. This is because the h_{ie} of the transistors depends on the emitter current . Therefore, when v_1 and v_2 are applied

simultaneously, the "strength" of v_1 will determine how much v_2 is amplified. In other words, multiplication is obtained when the gain varies linearly with the magnitude of v_1. A more elaborate analysis is given in Appendix B.

Since the device is used as a power monitor, both inputs are connected together and a squaring circuit is obtained.

In Figure 3-9·2 the input voltage and output voltage are plotted on logarithmic graph paper. The response was measured at three different frequencies, namely ½, 1, and 1½ MHz. It was found that the response curves were straight lines with slopes of 1.98, 2.02 and 2.02, respectively. Also, they were found to practically coincide. Departure from the straight line occurs for the larger input signals; therefore, the output of the device should be limited to approximately 300 mV.

As can be seen in Fig. 3-9·2, the above-mentioned effect becomes more pronounced as the frequency is increased. Also, for very small input signals there is some deviation from the straight line. However, as this occurs only for relatively insignificant input levels (below 1½ mV), the effect can be ignored.

In order to make the amplitude of the squared signal (X^2) the same order of magnitude as that of the original signal (X), the multiplier is followed by an amplifier. Both stages are shown in Fig. 3-9·3. The amplifier is coupled directly to the negative-going output terminal of the multiplier. The stage has a voltage gain of 13.5 dB.

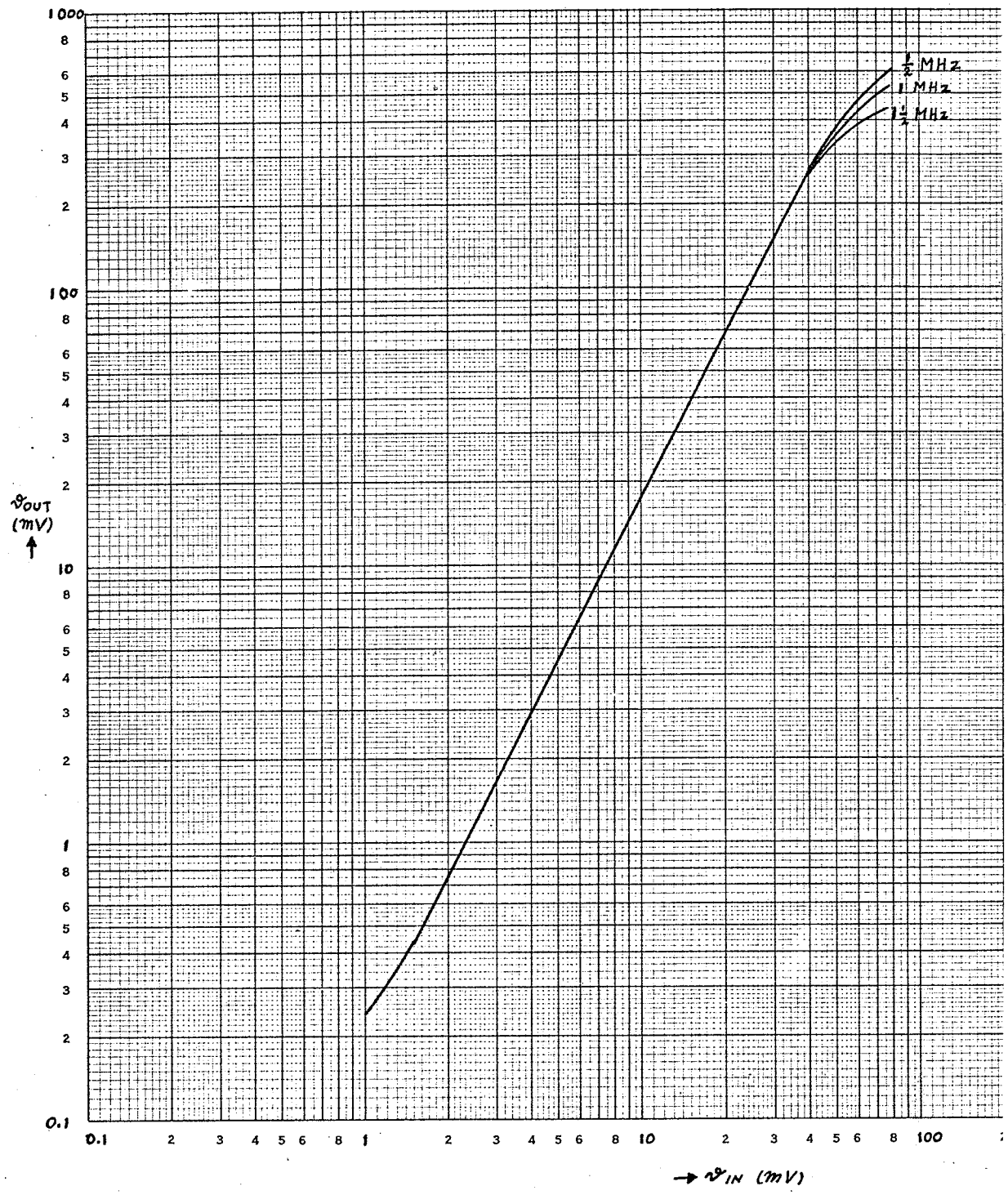

Fig. 3-9·2: MULTIPLIER TRANSFER CURVE

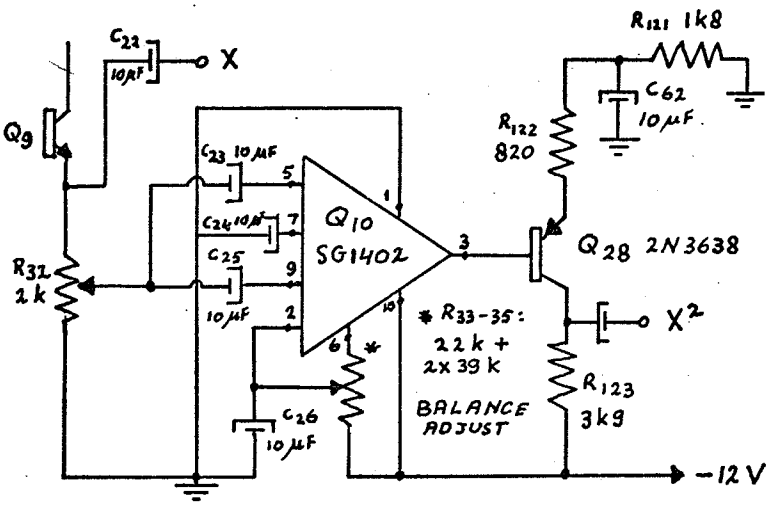

Fig. 3-9·3: MULTIPLIER AND AMPLIFIER CIRCUIT

3-10: Variable Threshold Amplifier

The circuit diagram of this stage is shown in Figure 3-10·1.

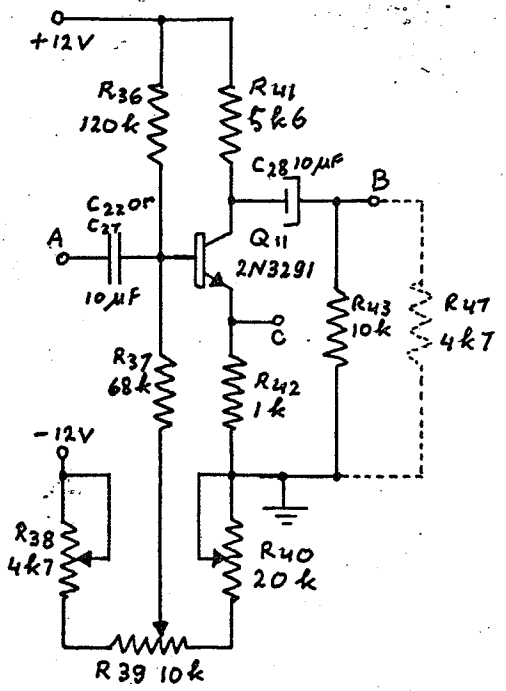

Fig. 3-10·1: VARIABLE THRESHOLD AMPLIFIER

A is the input terminal, and is connected either to the emitter-follower Q_9 (X) or to the amplifier succeeding the multiplier (X^2). Common-emitter

output terminal B is connected to the input of the averager (section 3-12) whose input impedance is represented by R_{47}. The emitter-follower output terminal C is connected to the comparator (section 3-11).

The threshold level is set by R_{39}, which controls the amount of reverse bias of the base-emitter junction of Q_{11} and can be varied between -1.7 volts (maximum threshold) and 0.6 volts positive, where the transistor is just forward biased (zero threshold).

The reason for the emitter follower output is twofold: the counting circuit is supplied with signals of the correct polarity, and the gain of the stage is made independent of the instantaneous emitter current, i.e. except for very small values of i_E. The h-parameter equivalent circuit of the stage is shown in Figure 3-10·2. Analysis of this circuit yields the following approximate expression for the voltage gain:

$$A = \frac{R_L}{r_e + R_E},$$

where only the term r_e depends on the emitter current and is given by $r_e = \frac{26}{i_E(mA)}$. Thus, the gain, A , does not depend on i_E, except for very small values of i_E.

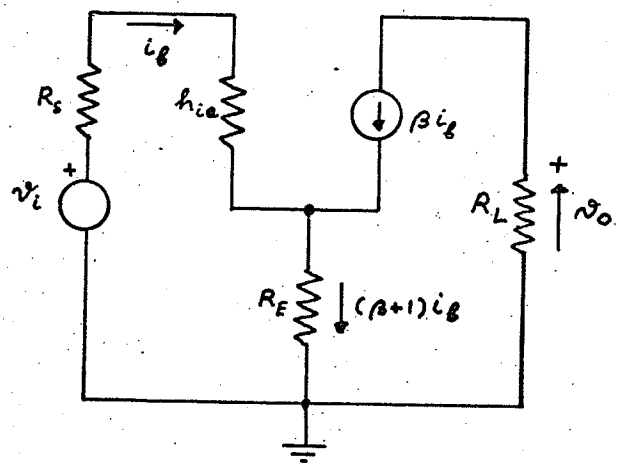

Fig. 3-10·2: EQUIVALENT CIRCUIT

3-11: Wave-Shaping Circuit, Comparator and Counting Monostable

Since an averager is available (see section 3-12), a convenient method for obtaining a count of the number of echoes that pass through the variable threshold amplifier is to convert them to pulses of constant width and amplitude. These pulses are subsequently averaged, and the average value obtained is directly proportional to their number (in one cycle).

The pulses are generated by a monostable. However, to trigger this monostable a much larger signal is required than that available from the threshold amplifier. It should be remembered that the monostable has to generate one pulse for every peak appearing at the output of the threshold amplifier, however small it may be. This then requires an amplifier with a very high gain and one which is of the "non-saturable" variety. That is, even if a large peak is available, which will drive the amplifier into saturation, it should come out of saturation immediately after this peak has disappeared, so that the amplifier can respond properly to the succeeding peak. Therefore the obvious choice is a comparator, which, in fact, is a non-saturable operational amplifier.

The circuit is shown in Figure 3-11·1.

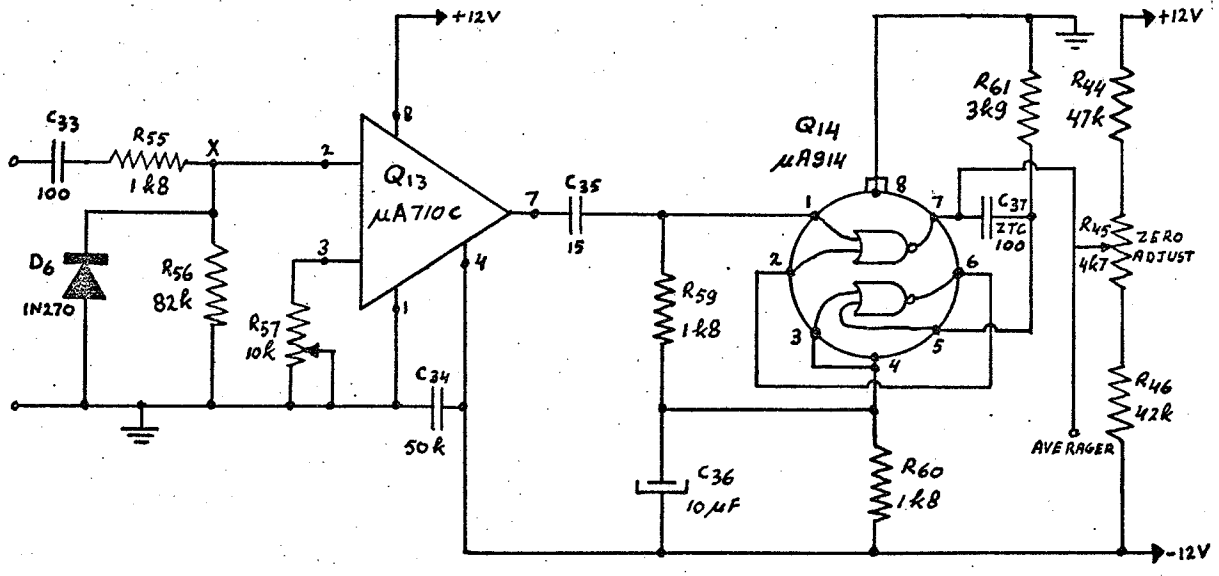

Fig. 3-11·1: COMPARATOR AND COUNTING MONOSTABLE

For the monostable we use an integrated dual NOR-gate, as it features low cost, small size, and requires few external components. The complete schematic diagram of the monostable is shown in Figure 3-11·2.

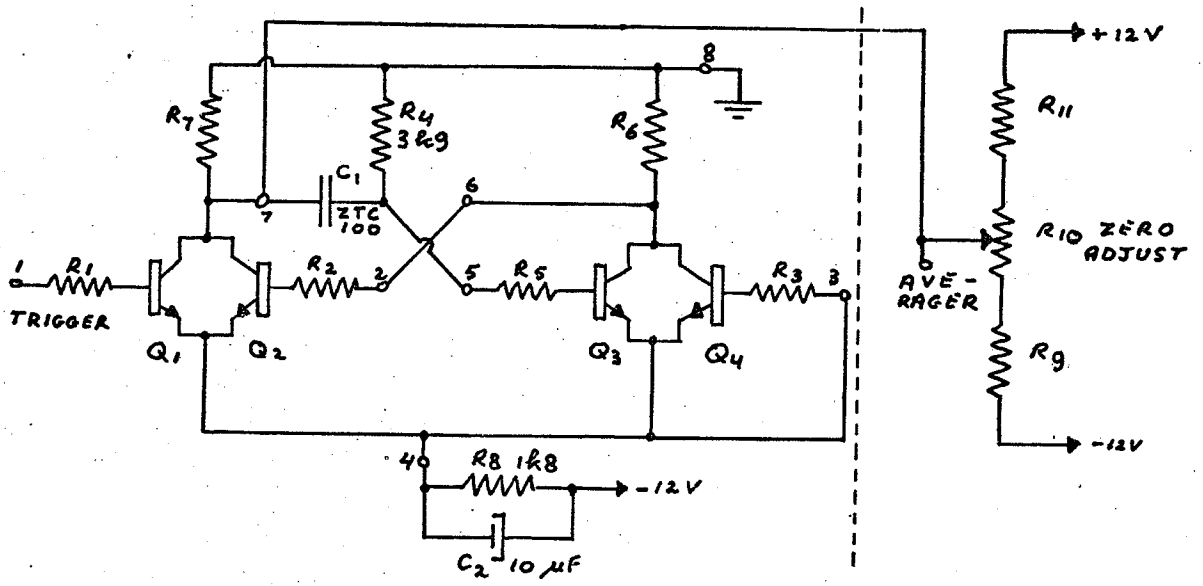

Fig. 3-11·2: DETAILED MONOSTABLE DIAGRAM

The actual monostable is drawn to the left of the dashed line. C_1, C_2, R_4 and R_8 are the only external components.

The pulse duration is determined by C_1 and R_4 and is fixed at 0.4 sec.

As the averager (see section 3-12) requires negative input signals to produce a positive output signal, we obtain the pulses from pin 7 where the voltage varies between zero and some negative value.

Figure 3-11·3 shows an example of the waveforms at various points in the counting circuit. The target at which the transducer was aimed was a peppercorn, immersed in water. The different traces show the following:

a) Envelope of the backscattered signal.

b) Output of the wave-shaping circuit (Point X in Fig. 3-11·1).

c) Output signal of the comparator Q_{13} (pin 7).

d) Pulses generated by the monostable.

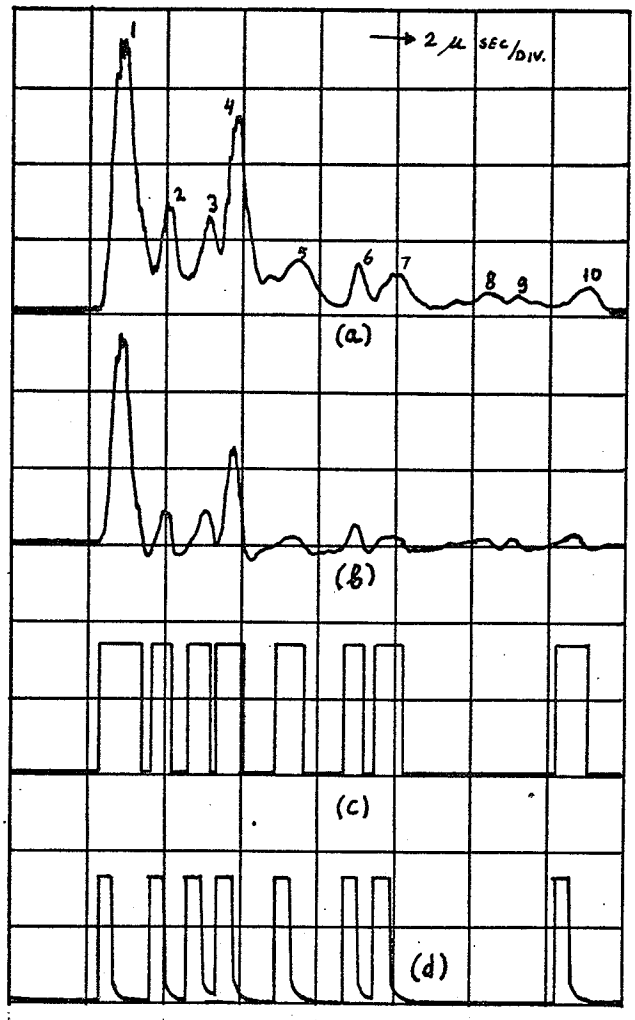

Fig. 3-11·3: WAVEFORMS IN THE COUNTING CIRCUIT

The requirement to be satisfied by the counting circuit is that the number of distinct echoes be determined - one pulse being generated for each such echo.

This is, of course, a somewhat arbitrary requirement, since it is not always clear what constitutes a distinct echo. The best "criterion" is established by visual inspection of the backscattered signal.

Referring to Figure 3-11·3(a), we would conclude that the peaks 1 through 7 and 10 would qualify, whereas 8 and 9 would not be considered

distinct. Whether the two together should be regarded as one echo is also very debatable, considering the low amplitude (compared with the other peaks) and the low rates of change.

The wave-shaping circuit, which is redrawn in Figure 3-11·4, does not discriminate between pulses 8 and 9, nor does the composite pulse produce a response sufficient to make the comparator change state.

The necessity for the wave-shaping circuit becomes clear when we recall how the comparator operates: if the signal of Figure 3-11·3(a) were applied to the comparator, its output would change state at the beginning of the first peak and remain in the high state until after peak 10, since the signal is positive everywhere in between.

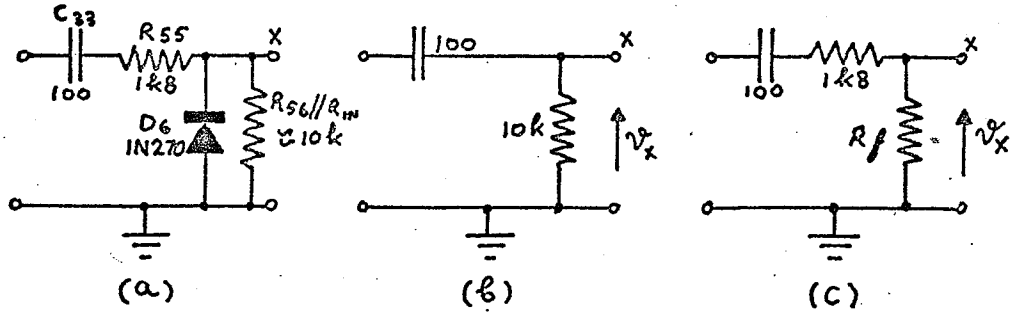

Fig. 3-11·4: (a) COMPLETE CIRCUIT

(b) EQUIVALENT CIRCUIT FOR POSITIVE v_x

(c) EQUIVALENT CIRCUIT FOR NEGATIVE v_x

The wave-shaping circuit, the component values of which were experimentally determined, operates as follows:

The positive going portion of a peak causes a positive signal at the output terminal X. This makes the comparator change state, and the monostable is triggered.

The negative-going portion of a peak tends to pull the output

voltage v_x down to zero, or even slightly negative, even if the peak itself does not completely return to zero. The reason is that the circuit behaves like an imperfect differentiator. The comparator now returns to its low state, and the circuit is ready to register the next peak. For a positive-going signal, the time constant is sufficiently large so that a considerable portion of the input signal appears at the output. When v_x becomes negative the diode conducts, giving the circuit a small time constant. This causes the capacitor to charge up very quickly, which, together with the voltage division across R_{55} and the diode forward resistance R_f, causes v_x to remain essentially at zero until the next positive going signal appears at the input.

As we can see in Figure 3-11·3(c), the output signal of the comparator remains high as long as v_x is positive; we only require the monostable to be triggered when the output of the comparator changes from zero to positive. Therefore, the monostable is coupled to the comparator via the differentiating network consisting of R_{59} and C_{35}.

The monostable output signal is shown in Figure 3-11·3(d).

3-12: Averager and Clamping Circuit

The output signal v(t) of the variable threshold amplifier appears across R_{43}. It is a repetitive waveform with a period of T sec. The signal is shown in Figure 3-12·1.

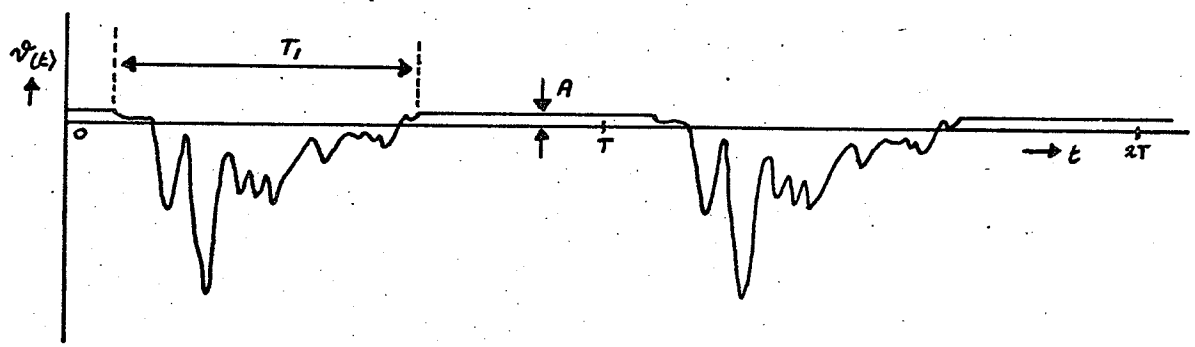

Fig. 3-12·1: OUTPUT SIGNAL, v(t), OF THE VARIABLE THRESHOLD AMPLIFIER

The D.C. component has been removed from the signal due to the coupling capacitors connecting the various stages. This means that the average value of v(t) is equal to zero and that the original baseline, which was at zero volts, has been shifted up by a certain amount A. The negative portion of v(t) has a maximum duration of T_1 seconds, whereas the minimum duration of the positive portion is equal to $T-T_1$. Since T_1 is very much smaller than T (typical figures are 10 μsec and 1000 μsec, respectively), we may conclude that the level difference A will be very small compared to the absolute value of the average signal level in the time-interval T_1. Therefore, rectifying the signal of Figure 3-12·1 and retaining the negative part is essentially equivalent to restoring the original baseline, or, in other words, clamping the signal to the level of zero volts.

The signal can now be fed into the averager to produce the average value of v(t) in the time-interval T, or, equivalently, the time-integral of the signal over that interval. The average signal in the time-interval T_1 can now be found by multiplying the output signal of the averager by T/T_1. The amplitude of v(t), as a function of time, may be obtained by selecting a narrow[1] window (of known width) and moving this window along the time-axis.

Averaging is accomplished by the operational amplifier circuit of Figure 3-12·2. The voltage transfer function of this circuit is given by:

$$A(s) = \frac{R_{53}}{R_t} \cdot \frac{1}{s\, R_{53} C_{31} + 1},$$

where R_t is equal to the sum of R_{47} and the output impedance of the preceeding stage. The second factor in the above expression will be

---

[1] Narrow in the sense that relative changes of the signal within the window are small.

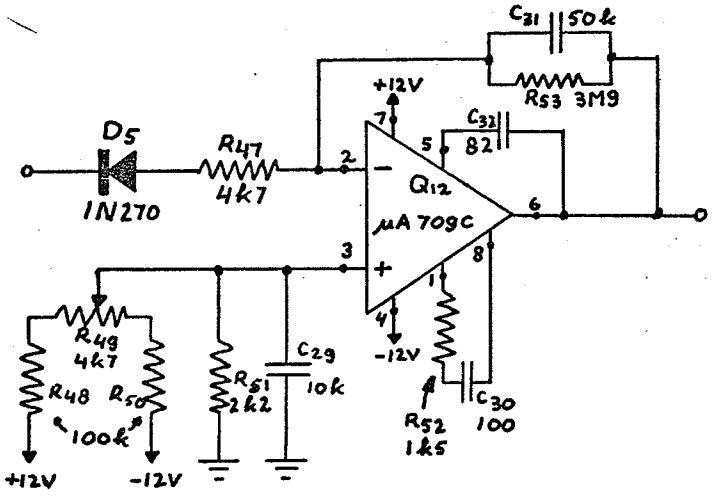

Fig. 3-12·2: AVERAGING AND CLAMPING CIRCUIT

recognized as being the transfer function of a low-pass R-C filter, a well-known averager. The first factor provides the gain required for an output signal of the order of a few volts, which, together with the current-drive capability of the operational amplifier, allows the meter, as well as other monitoring equipment, to be connected without disturbing the output level. The components C_{30}, R_{52} and C_{32} provide frequency compensation. The potentiometer R_{49} is used to adjust the output voltage to zero when the input voltage is equal to zero. Diode D_5 is the "clamping" diode.

To check the performance of the averager, three tests were performed.

a) A square wave of constant repetition frequency (1 kHz) and constant width (10 μsec) was applied to the input, and the amplitude was varied between 0 and 1750 mV. The result is shown in Figure 3-12·3(a). The response curve is quite linear and has a slope of 7.2. The calculated value of this slope is 8.3, and the difference is due to the leakage resistance of capacitor C_{31}.

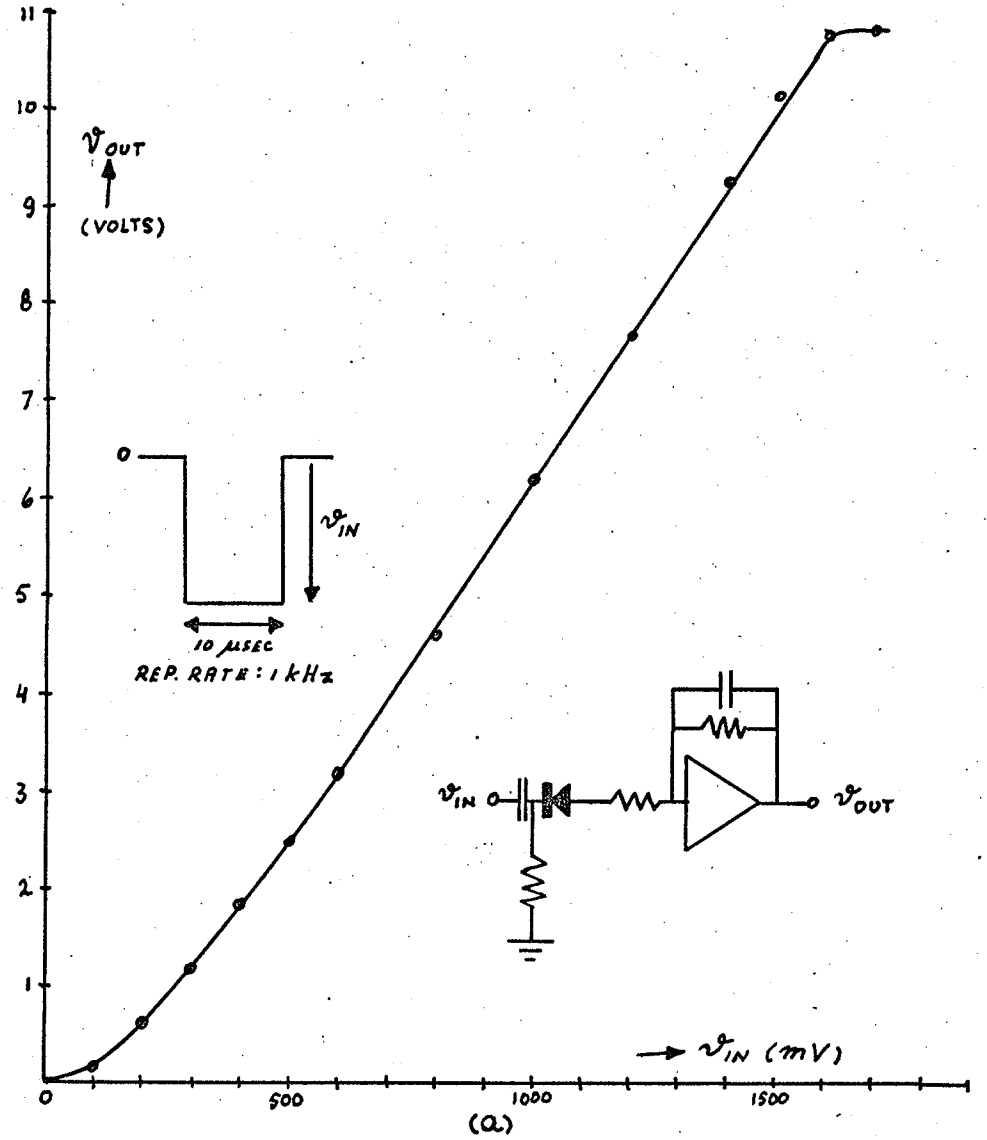

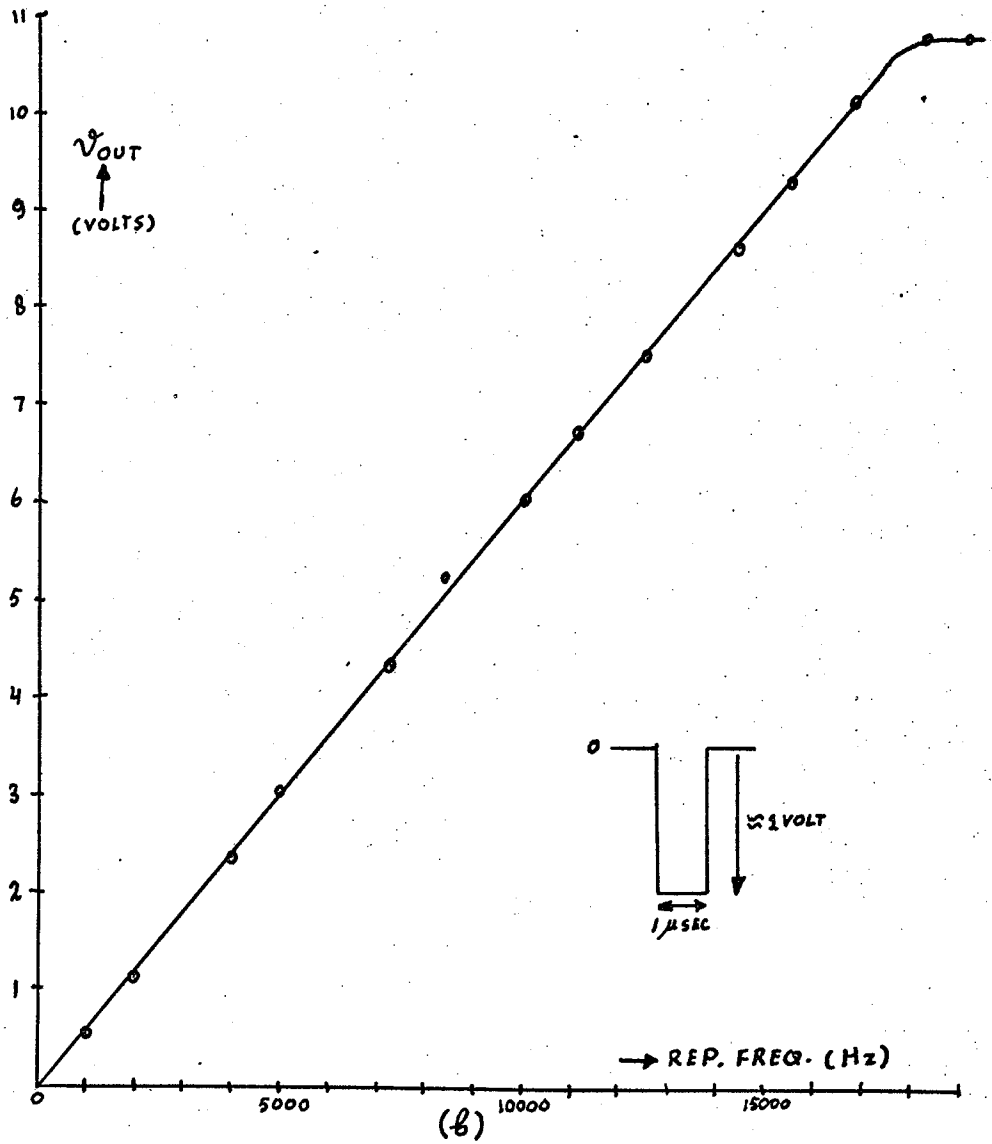

FIG. 3-12-3: (a) RESPONSE TO VARYING AMPLITUDE

(b) RESPONSE TO VARYING REPETITION FREQUENCY

For low input voltages the off-set due to the diode can be observed. As the amplitude is increased, a point is reached where the operational amplifier saturates. The saturation output voltage is 10.75 volts.

b) A square-wave of constant width (1 μsec), constant amplitude (approximately 1 volt), and varying repetition frequency was next applied to the input. The response is extremely linear as can be seen from Figure 3-12·3(b).

c) To investigate the behaviour for different frequencies, a sinusoidal signal was applied, which, of course, was rectified by the diode. The frequency was varied from 250 kHz to 2 MHz. It was found that the response drops off (approximately 2½% at 2 MHz) only above, approximately, 1.5 MHz.

3-13: Reference Monostable and Ramp generator

The purpose of the reference monostable is to provide a pulse of constant width and amplitude. Depending on the mode of operation (contact or immersion), it is triggered once every cycle, either by the trigger oscillator (at t=o), or, after some delay, by the gate-pulse monostable. The pulse obtained is used for two purposes:

1. It is integrated to give a ramp which controls the variable gain amplifier. The amplitude has to be constant, since the slope of the ramp is directly proportional to this amplitude.
2. The pulse can be fed into the averager, which will thus give us an indication of the repetition rate of the system, provided that both width and amplitude of the pulse are constant.

The circuit diagram is shown in Figure 3-13·1. The monostable is emitter-coupled and consists of transistors Q_{15},Q_{16} and their associated components. A positive trigger signal is applied to the base of Q_{15} which

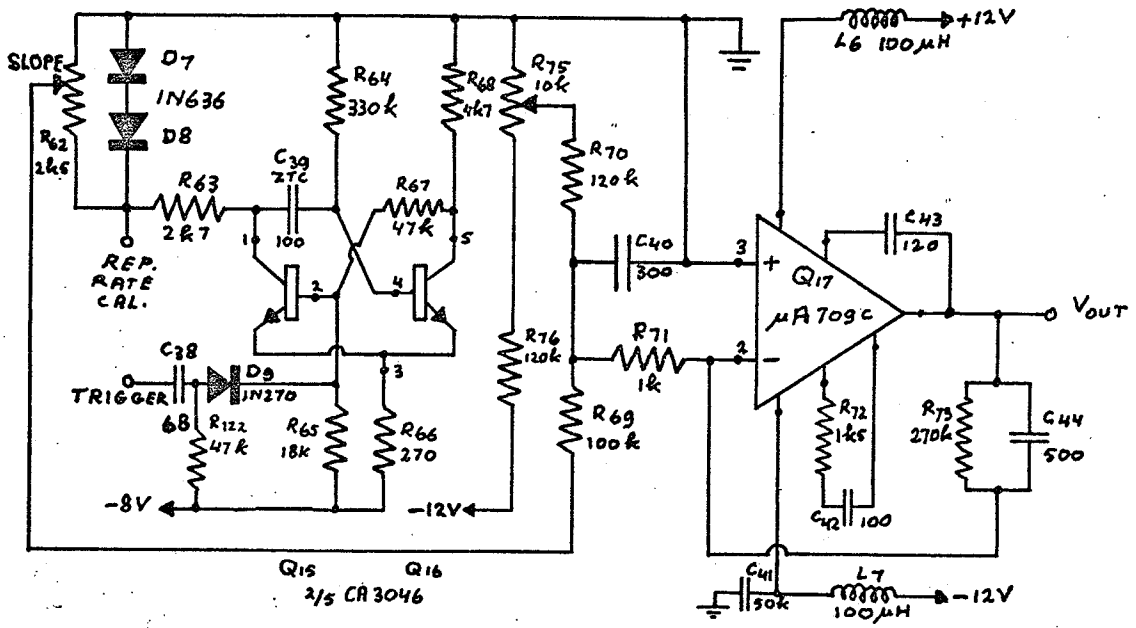

Fig. 3-13·1: REFERENCE MONOSTABLE AND RAMPGENERATOR

is made to switch from its OFF-state to its ON-state.

Part of the collector pulse of Q_{15} appears across the diodes D_7 and D_8, which help to provide us with a signal of constant amplitude. The type of diode used (1N636) has a sufficiently large offset voltage, so that only two of them are required to produce a large enough pulse. The timing capacitor has zero temperature coefficient, to provide a pulse of constant width. As the monostable shares its trigger source with another monostable, the diode D_9 has been included to avoid interaction between them.

The ramp generator cicuit is essentially the same as the averager circuit discussed in the previous section. The only differences are that the output frequency compensation capacitor was increased from 82 pF to 120 pF (C_{43}) to increase the linearity of the ramp, while the components in the feedback loop have different values. The non-linearity caused by R_{73}, which is required for the output signal to return to its original level (before the input pulse was applied), is offset by capacitor C_{40}. The slope of the ramp, obtained through integration of the square pulse generated by the monostable, is controlled by potentiometer R_{62}, the slope being proportional to the amplitude of the pulse. The D.C. output level of the ramp generator (V_o D.C.) is controlled by potentiometer R_{75}. The output signal is shown in Figure 3-13·2.

Here T_p is approximately 25μsec and much smaller than T. The time constant $R_{73}\cdot C_{44}$ has to be so small that the output voltage returns to V_o D.C. just before triggering, independent of the slope (tan). Components L_6, L_7 and C_{41} were necessary for power supply decoupling, as the operational amplifier had a tendency to oscillate when connected directly to the power supply. For the design procedure of the monostable in this section and the ones in the following section, we refer to an

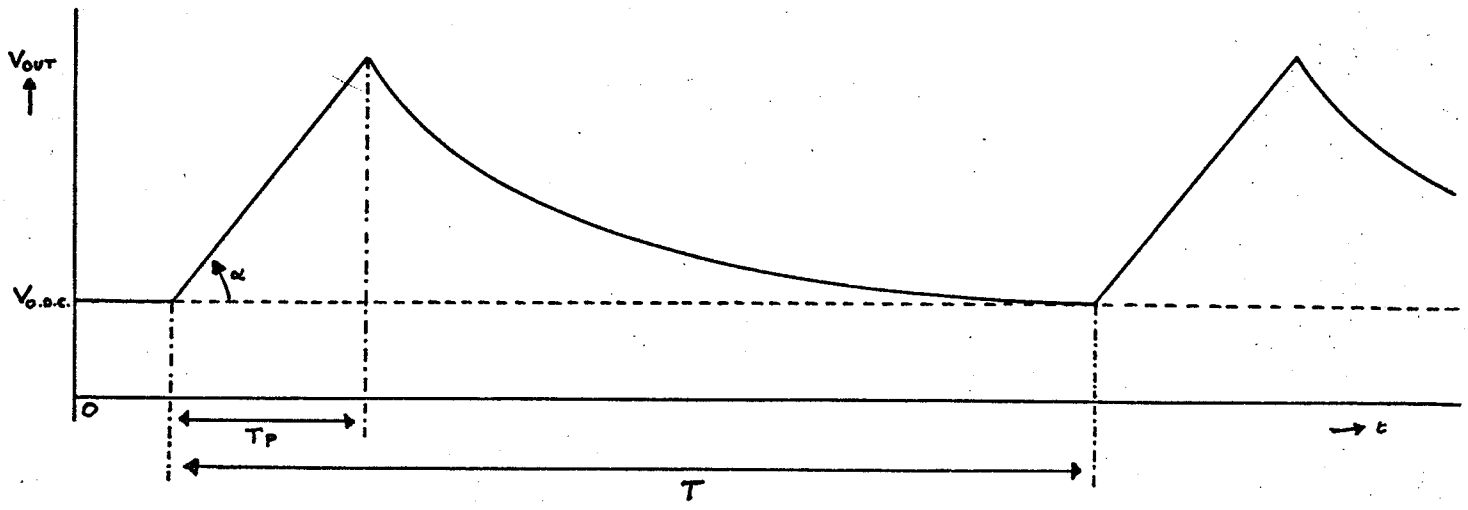

Fig.3-13·2: OUTPUT OF THE RAMPGENERATOR

article by R.S. Hughes entitled: "Get the Facts on One-Shot Design".[7]

3-14: Delay and Gate Pulse Monostables

The delay monostable determines the time that elapses between transmission and opening of the gate. The gate pulse monostable determines how long the gate will remain open. The complete circuit, shown in Figure 3-14·1, contains two more stages: a trigger amplifier (Q_{28}), which ensures stable triggering under all conditions, and an inverter (Q_{20}), necessary because the gate pulse monostable (Q_{21}-Q_{22}),which requires positive triggering, must respond to the trailing edge of the delay monostable output. Both delay monostable (Q_{18} - Q_{19}) and gate pulse monostable (Q_{21}-Q_{22}) are emitter-coupled like the previously discussed reference monostable. The only difference is that they cover a different range of pulse widths: 2.5 ÷ 25 μsec (delay monostable), and 1.5 ÷ 25 μsec (gate pulse monostable). The minimum pulse width of the delay monostable is larger because we can never receive a meaningful signal until after the transmitter has stopped ringing entirely. Also, in case of fish testing,

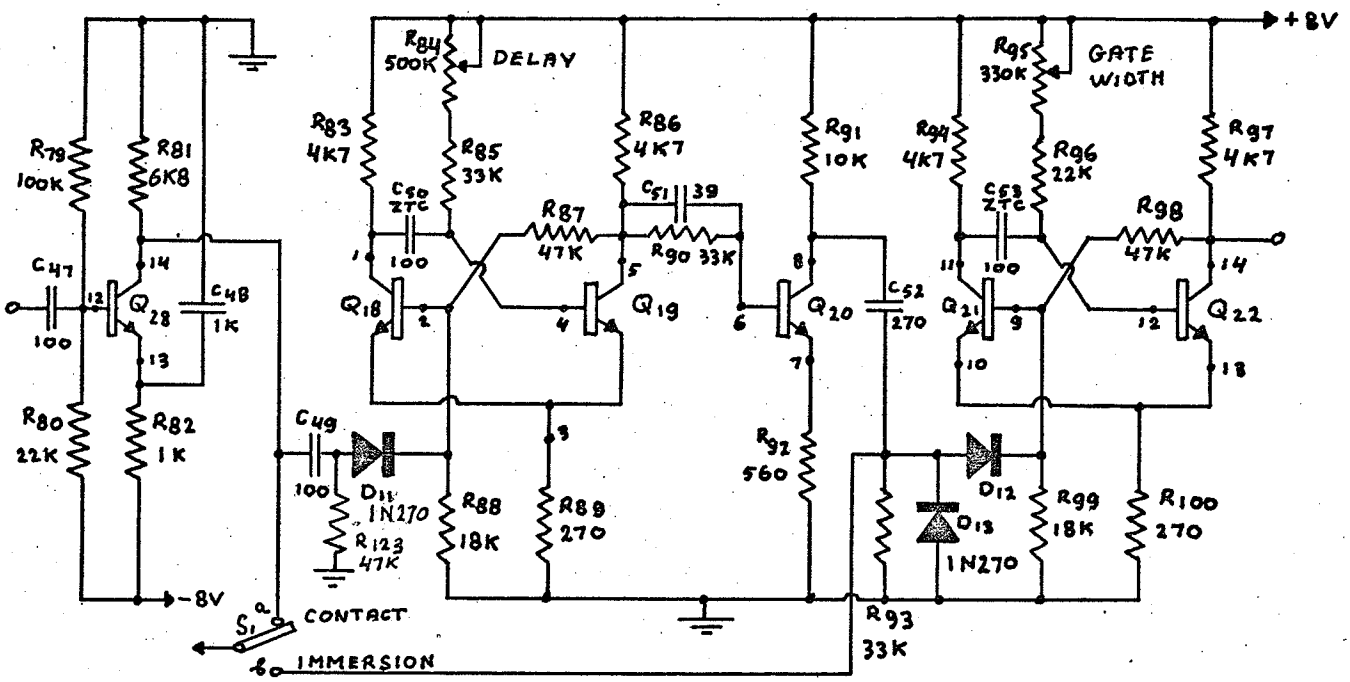

Fig. 3-14·1: TIMING CIRCUITS

we are not interested in the signals due to the skin reverberation. As can be seen in the diagram, the reference monostable may be triggered simultaneously with the transmitter (S_1 in position a), or together with the gate-pulse monostable (S_1 in position c).

The diodes D_{11}, D_{12} and D_{13} prevent interaction between the various monostables.

3-15: Power Supply

The power requirements of the analyzer are: 50 mA at plus and minus 12 volts, and plus 300 volts for the pulser, which draws a negligible amount of current (0.084 Asec times the repetition rate). All voltages are regulated.

The circuit diagram is shown in Figure 3-15·1. The transformers T_2 and T_3 were chosen for minimum size, weight and cost. No commercially-available single transformer was found which satisfied all requirements,

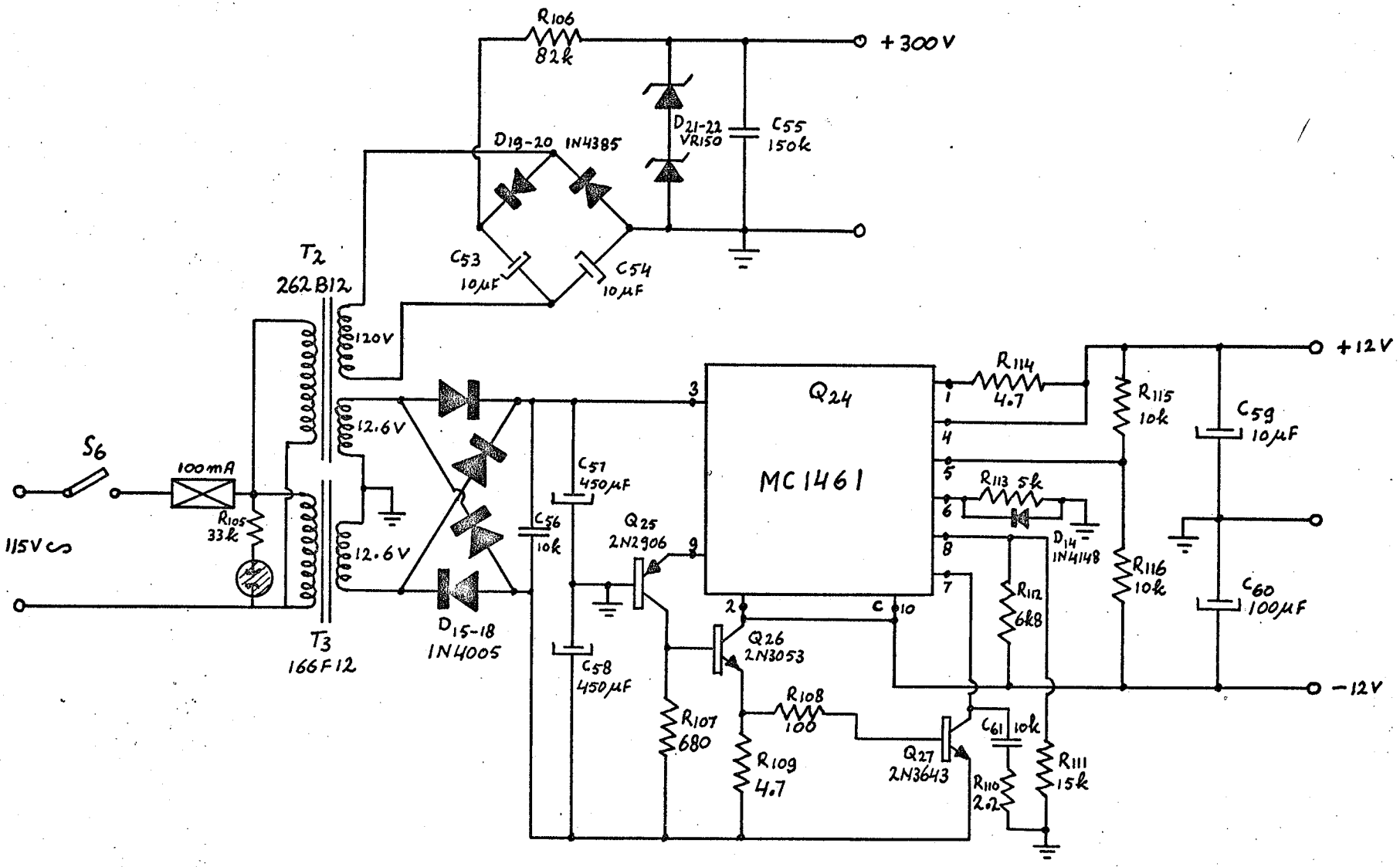

FIG 3-15·1: POWER SUPPLY

and hence, two transformers are used.

Diodes D_{19}-D_{20}, together with capacitors C_{53}-C_{54} form a voltage doubler. The voltage is approximately held constant at 290 volts by the Zener diodes D_{21}-D_{22}, whose power dissipation is limited by resistor R_{106}. For a line-voltage change from 92 volts to 138 volts (115 V ± 20%), the output voltage changes by 4.5 volts (at a repetition rate of 450 Hz), which corresponds to a regulation of 0.35%. Line regulation is defined as $\frac{1}{V_{out}} \cdot \frac{V_{out}}{V_{line}} \times 100\%$.

The measured values of the other supply voltages are: $V^+ = 11.5$ volts and $V^- = -11.6$ volts. These values are extremely constant, V^+ down to a line-voltage of 92 volts (r.m.s) and V^- down to 83 volts (r.m.s.)

The values of V^+ and V^- where chosen somewhat below ± 12V, so as not to exceed the maximum voltage ratings of some of the integrated circuits.

3-16: Meter

The meter that was chosen is a taut band, mirror scale panel meter with dimensions 130 mm. x 102 mm. (5.10" x 3.96"). The scale is linear, and calibrated in microamperes, 100 μA corresponding to full scale reading. Further specifications are: accuracy ± 2%, tracking ± 1.5%, and repeatability ± 0.5%. The scale length is 107 mm. (4.22").

It is, of course, possible to make different scales for the various modes of operation. However, the calibration of these scales depends on the final calibration of the complete instrument, which in turn may depend on the particular application. It is therefore recommended not to introduce these specialized scales until after some experience has been obtained with the analyzer.

The meter is used essentially as a voltmeter, measuring the output

voltage of the averager. Consequently, it causes negligible loading of the operational amplifier. The sensitivity can be controlled with potentiometer R_{54}.

3-17: Miscellaneous

Various points in the circuit may be monitored. It is also possible to feed in external signals for processing. The test points, which are indicated in the diagrams of section 3-18, are:

A: Output of the pre-amplifier Q5.

B: Input of the amplifier Q7.

C: Output of the emitter-follower Q9.

D: Output of the amplifier Q28 (following the multiplier).

E: Input of the averager.

F: Output of the counting monostable.

G: Output of the averager.

J: Output of the ramp generator.

K: Output of Q23 (gate pulse).

L: Output of Q20 (delay pulse).

Test points A through G may be connected to a BNC connector via a multi-position switch. Points J, K and L each have their individual connectors.

The repetition rate calibration switch (S4) has two sections. Section b connects the output of the reference monostable to the input of the averager via the divider network consisting of resisitors R103 and R104. The value of R104 can only be selected after the final calibration of the instrument, i.e. after R54 has been fixed.

3-18: Complete Circuit Diagrams

The complete circuit diagrams of the analyzer are shown on the next three pages.

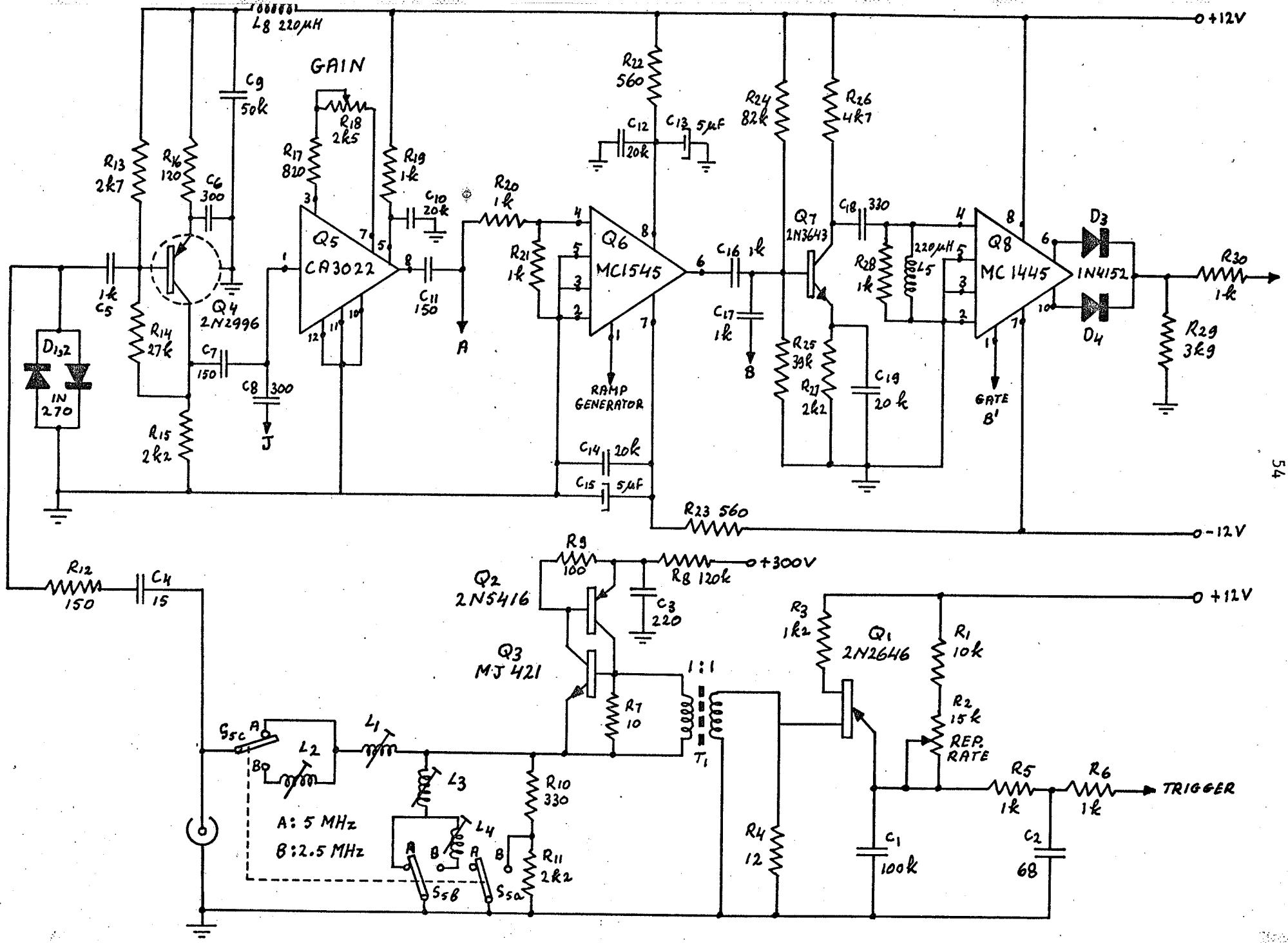

FIG. 3-18.1: PULSER- AND R.F. CIRCUITS

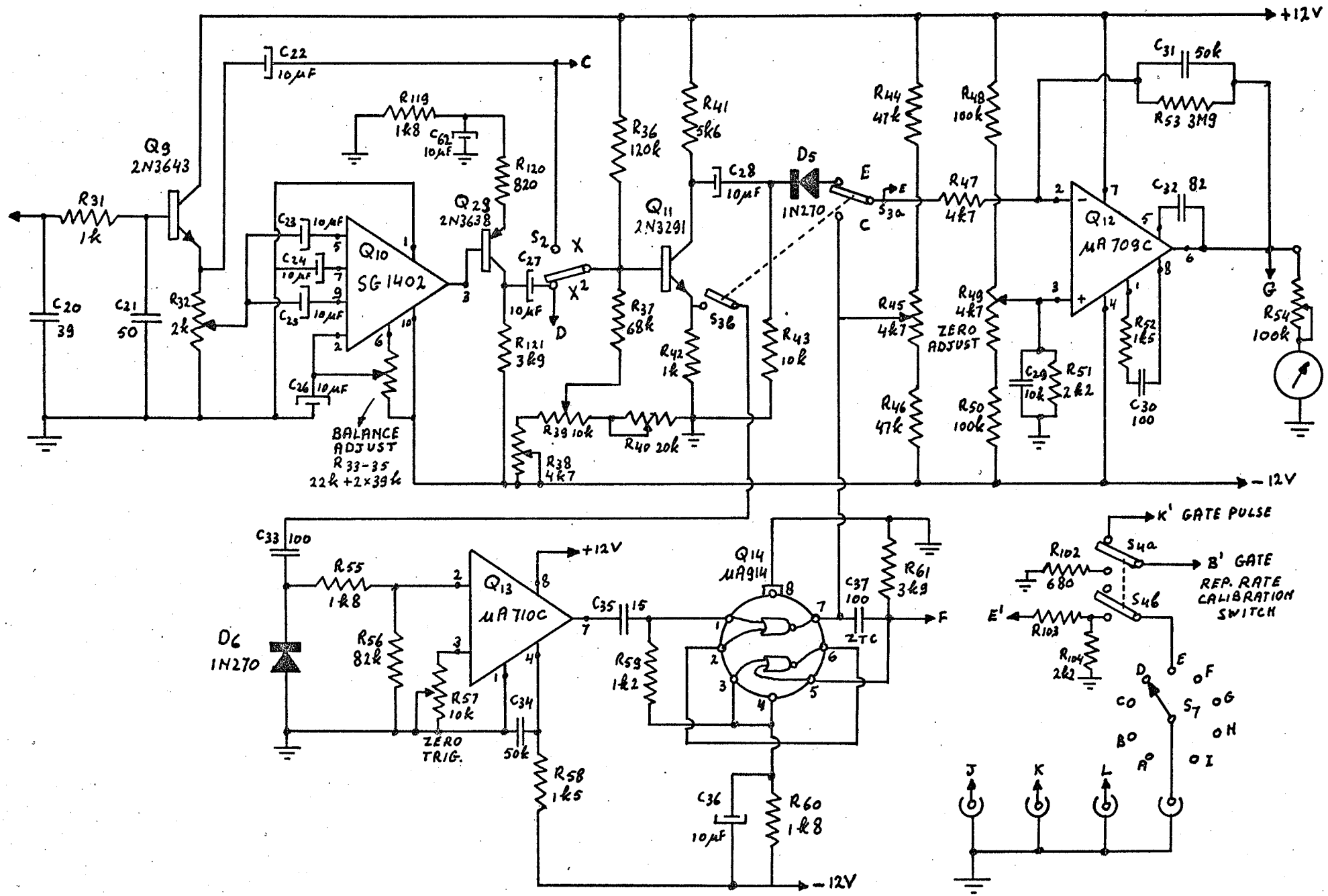

FIG 3-18·2: VIDEO- AND OUTPUT CIRCUITS

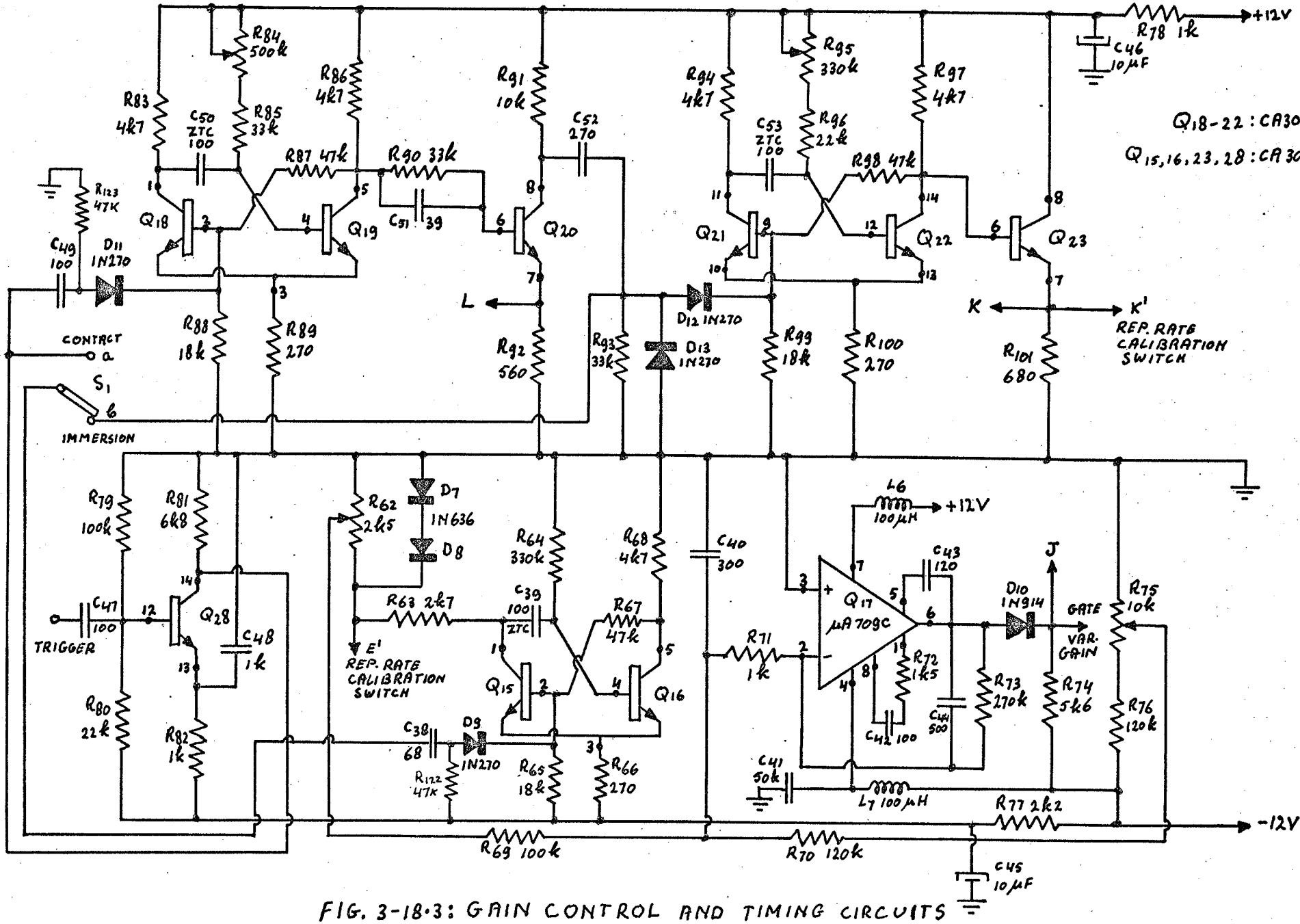

FIG. 3-18-3: GAIN CONTROL AND TIMING CIRCUITS

CHAPTER IV

RESULTS OF FISH TESTS

The analyzer was developed primarily for the determination of the freezing temperature of fish tissue. Therefore, a good criterion for its satisfactory operation is whether or not the measurements, performed on samples which have been frozen at different temperatures, reveal the differences in the freezing history. Even with complete knowledge of the backscattered signal, it requires considerable experience to be able to estimate the original freezing temperature of a sample. Therefore, the test procedure chosen was as follows: a series of three to five measurements (at 5 MHz) were performed on four fish which had been frozen at -10, -20, -30 and -40 ^{o}C. The measured results were averaged for each sample and the standard deviation was determined for the measurements of the average amplitude and average power. Next, someone, experienced in estimating freezing temperatures from A-scan analyses, was asked to interpret the data. The estimates were then checked against the records of the Fisheries Research Board (F.R.B.) laboratory, and it was found that all four estimates were correct. It should be pointed out that only rough estimates can be made, no matter which method is used; it cannot be expected that one can distinguish between samples having a difference in freezing temperature of only a few degrees.

The measurement procedure for each sample was as follows: the sample was thawed and the scales were removed from an area of about 4x7 cm, so that measurements could be made at a few different locations. Removal of the scales is not essential, but it decreases the attenuation. The sample was next immersed in water and the transducer was positioned at a distance of

approximately 2 cm from the surface of the sample, with its axis perpendicular to the surface. A gain setting was chosen which produced sufficiently large signals, and, in addition, a variable gain of 0.2 dB/ usec was introduced. The window was 15 microseconds wide, starting 4 microseconds after the beginning of the skin reverberation. The threshold level was set at zero.

Figures 4-1 and 4-2 show some of the signals obtained with samples 3 and 4, respectively. The traces are - from top to bottom:

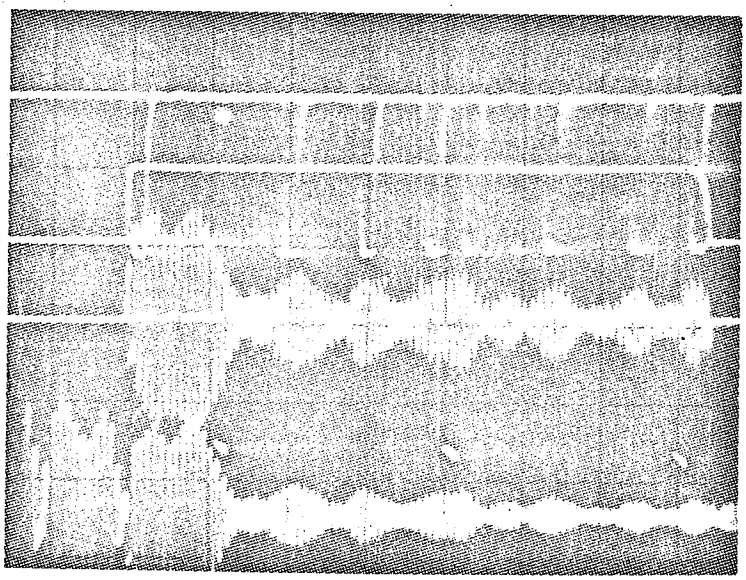

Fig. 4-1: SAMPLE 3

- Output of the counting monostable (counting echoes of $v_T(t)$),
- Gate pulse,
- Output of the gated amplifier,
- Input of the variable gain amplifier.

The measurement results are shown in Table 1. The designations C, E, X and X^2 refer to the position of the mode selector switches:

CX / count of the echoes in the signal,

EX / average amplitude of the signal,

EX^2/ average amplitude of the square of the signal (average power), and

CX^2/ count of the peaks in the square of the signal.

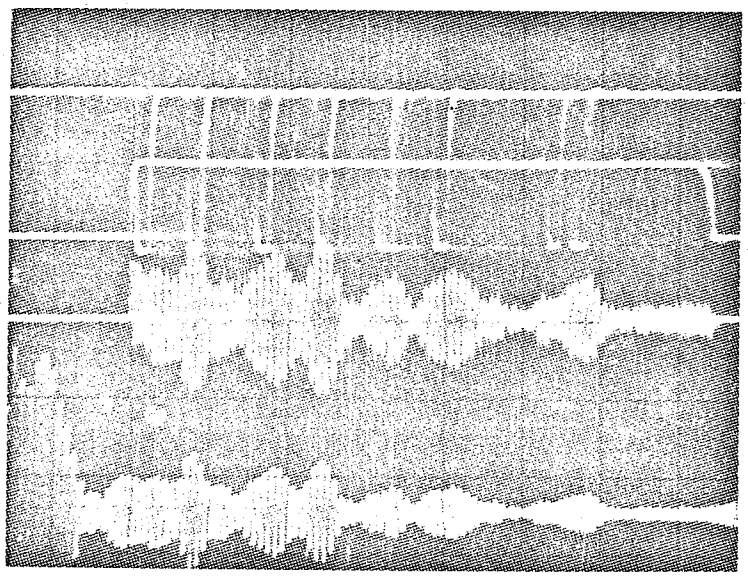

Fig. 4-2: SAMPLE 4

The gain setting chosen for sample 1 could be maintained for samples 2 and 3, whereas sample 4 required 11 dB less gain.

It should be noted that the sample numbers 1, 2, 3 and 4 were used for convenience, while the actual sample identification numbers (assigned by the F.R.B.-Lab.) were 55, 66, 59 and 69, respectively.

It can be seen from the Table that the count of the peaks of the squared signal is less than might be expected. The reason for lower readings in the column CX^2, as compared to the column CX, is that the average levels of X and X^2 were made compatible, so that in the case of X^2, the smaller peaks were greatly suppressed, and as a consequence, were not registered.

SAMPLE	FREEZING TEMPERATURE (°C)	GAIN SETTING (dB)	C X	E X	E X^2	C X^2
1	-40	23	52	48	51	45
			66	32	29	26
			58	33	30	23
			71	45	56	30
AVERAGE			58.7	39.5	41.5	31.0
STANDARD DEVIATION				5.0	12.2	
2	-30	23	94	63	41	37
			83	45	36	32
			80	64	49	37
AVERAGE			85.7	57.3	42.0	34.5
STANDARD DEVIATION				8.75	5.35	
3	-20	23	90	73	85	36
			81	43	31	27
			66	41	35	23
			93	77	75	57
			84	44	39	28
AVERAGE			82.8	55.5	53.0	37.0
STANDARD DEVIATION				15.9	22.4	
4	-10	12	95	59	46	46
			83	67	53	52
			88	61	51	28
			86	66	69	53
AVERAGE			88.0	63.3	51.2	44.7
STANDARD DEVIATION				3.36	9.1	
			ARBITRARY		UNITS	

TABLE 1: MEASUREMENT RESULTS

CHAPTER V

DISCUSSION AND CONCLUSIONS

The ultrasound backscatter analyzer which has been described makes it possible to obtain in an easy and quick manner the data necessary for the determination of the freezing temperature of fish tissue.

The development of the analyzer was based on the discovery made by Freese and Makov that there exists a correlation between the nature of the backscatter from thawed fish tissue and the temperature at which this tissue had been frozen (if at all).[1]

The main advantage of the instrument is that measurements of the average amplitude, power, and the number of echoes (in a selected time interval) are obtained as a meter indication in negligible time. This is in contrast to the previously employed technique whereby photographs of A-scan oscilloscope traces had to be analyzed manually - a time consuming and tedious process. The test results - determination of the freezing temperatures of four samples - were obtained in two hours, whereas, using the old technique, the required time for testing and analysis would be close to two weeks.

A two-transistor switch is used to discharge a capacitor into a ceramic transducer, causing it to generate bursts of high-frequency mechanical vibrations. The advantage of the two-transistor switch over a more conventional silicon controlled rectifier lies in the fact that higher switching speeds can be obtained.

Variable gain allows compensation for the absorption in the propagating media. The integrated cicuit used for this purpose, while providing adequate gain variation, has the disadvantage that a significant

---

[1] patent applied for - this technique was first described in a Report of an Invention under the Public Servants Act (unpublished)

amount of noise is introduced. This is because, in order to cover the desired range of gain, the device must be biased to give an initial gain of -40 dB. A possible solution to this problem might be to use recently developed low-frequency PIN-diodes.

Finally, the analyzer meets the requirements of portability and meter indication of the measured quantities, and thus it should prove to be a useful tool in the research of ultrasound backscatter phenomena.

B I B L I O G R A P H Y

[1] Freese, M. and Makov, D., "High-Frequency Ultrasonic Properties of Freshwater Fish Tissue", J. Acoust. Soc. Amer. 44 (5), pp. 1282 - 1289, 1968.

[2] Freese, M. and Makov, D., "Ultrasound Backscatter in Fresh and Thawed Animal Tissue", J. Fish. Res. Bd. Canada, 25(3), pp. 605 - 606, 1968.

[3] General Electric Transistor Manual, pp. 310 - 313, 1964.

[4] Beroza, P. P., "R. F. Burst Discharge from Tuned Circuits", The Electronic Engineer, March, 1967.

[5] Motorola, Specification Sheet DS 9117, Jan., 1969, and Application Note Al 475.

[6] Silicon General, Technical Bulletin 1402, 1970.

[7] Hughes, R. S. "Get the Facts on One-Shot Design," Electronic Design, Vol. 2, Jan., 1969.

[8] Millman, J. and Taub, H., Pulse, Digital and Switching Waveforms, McGraw - Hill, pp. 460 - 466, 1965.

****

APPENDIX A

TWO-TRANSISTOR SWITCH

The characteristic of a two-transistor switch together with the circuit diagram is shown in Figure A-1.

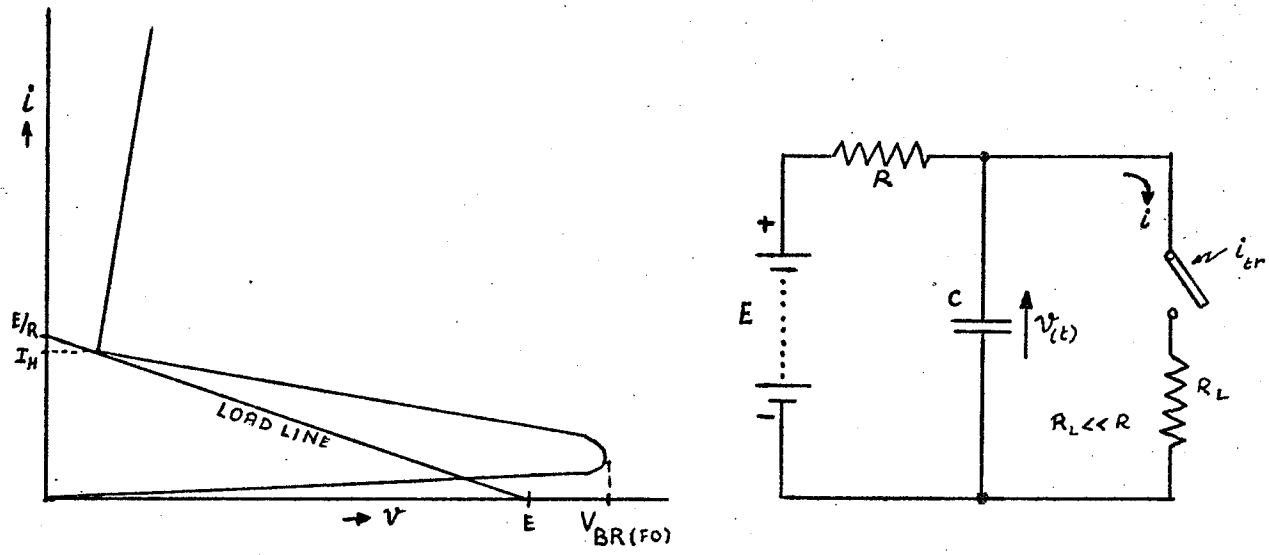

(a) (b)

Fig. A-1: (a) DEVICE CHARACTERISTIC

(b) EQUIVALENT CIRCUIT DIAGRAM

If the switch is to turn off after having been triggered, E/R must be less than the holding current I_H (assuming $V_H \ll E$). This means that the load line should lie below the point (V_H, I_H).

Also, to avoid the occurence of rate-effect, E/RC must be less than the forward voltage application rate (A) of the switch. The maximum voltage that can then be developed across the switch in a time interval T is given by:

$$v_{(T)_{max}} = ET/RC = AT \ .$$

This is achieved by increasing E and R in such a manner that E/R remains constant and less than both I_H and AC.

Also, E should be chosen below the forward breakdown voltage $V_{BR(FO)}$

unless the time interval between subsequent trigger pulses is short enough to prevent the capacitor voltage from exceeding $V_{BR(FO)}$.

Summarizing, we have the following conditions for proper operation of the switch:

$$E/R < I_H \qquad \text{(device can turn off)},$$

$$E/R < AC \qquad \text{(no rate-effect), and}$$

$$E < V_{BR(FO)} \qquad \text{(no self-triggering)}.$$

The measured values of the holding current (I_H) and the forward breakdown voltage ($V_{BR(FO)}$) were 270 mA and 450 volts, respectively. The current at the breakover point was 9 mA. The forward voltage application rate (A) was found to be extremely high, and it did not have to be considered in the design.

A final consideration is that if the repetition period (T) is variable, then the capacitor voltage just before triggering will, in general, increase with increasing values of T. As long as the time constant RC is much smaller than the minimum repetition period, then $v_{(T)}$ is essentially independent of this period.

In our application the time constant is 26 microseconds, whereas the repetition period may vary between 1 and 2 milliseconds.

The value of resistor R was chosen to satisfy all conditions.

APPENDIX B

MULTIPLIER ANALYSIS

The circuit diagram of the multiplier is redrawn in Fig. B-1 (a). The small-signal h-parameter model is shown in Fig. B-1 (b).

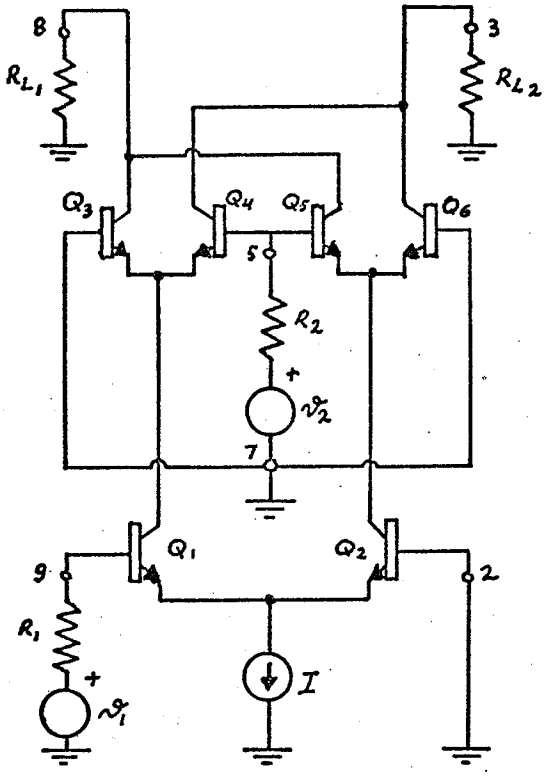

Fig. B-1 (a): CIRCUIT DIAGRAM

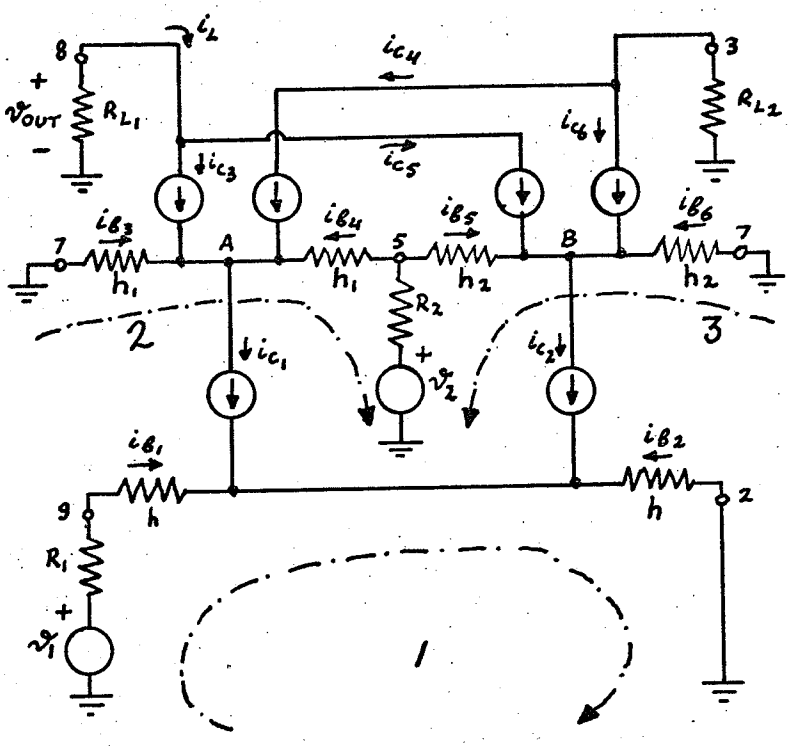

Fig. B-1 (b): h-PARAMETER MODEL

The constant current source, I, does not appear in the incremental model, as it has an infinite dynamic impedance.

The following assumptions are made:

a) The collector current $i_{C1} = I_{C1} + i_{c1}$ is divided equally between transistors Q_3 and Q_4; similarly, the collector current $i_{C2} = I_{C2} + i_{c2} = I_{C1} - i_{c1}$ is divided equally between transistors Q_5 and Q_6.

b) The various base currents (ib_3 - ib_6) are assumed to make no contribution to the corresponding emitter currents.

The corrolary of assumptions a) and b) is that

$$h_{ie3} = h_{ie4} \equiv h_1, \text{ and}$$

$$h_{ie5} = h_{ie6} \equiv h_2.$$

c) Finally, it is assumed that $h_{ie1} = h_{ie2} \equiv h$, and that the forward

current gains of all transistors are identical, and equal to h_{fe}.

Applying Kirchhoff's voltage law to loops 1, 2 and 3, and Kirchhoff's current law to nodes A and B yields the following set of linear equations:

$$\begin{bmatrix} 1 & 1 & o & o \\ o & o & 1 & 1 \\ h_1 & -(R_2 + h_1) & -R_2 & o \\ o & -R_2 & -(R_2 + h_2) & h_2 \end{bmatrix} \begin{bmatrix} ib_3 \\ ib_4 \\ ib_5 \\ ib_6 \end{bmatrix} = \begin{bmatrix} ib_1 \\ -ib_1 \\ - v_2 \\ - v_2 \end{bmatrix} \qquad (1)$$

Solving equation (1) for iC_3 and iC_5 we obtain:

$$ib_3 = \frac{-v_2 h_2}{R_2 (h_1 + h_2) + 2 h_1 h_2} + \frac{ib_1}{2}, \text{ and}$$

$$ib_5 = \frac{v_2 h_1}{R_2 (h_1 + h_2) + 2 h_1 h_2} - \frac{ib_1}{2}.$$

The load current, i_L, is given by $i_L = i_{c3} + i_{c5} = h_{fe} (ib_3 + ib_5)$ or,

$$i_L = h_{fe} v_2 \frac{h_1 - h_2}{R_2 (h_1 + h_2) + 2 h_1 h_2} \qquad (2)$$

In general, we may write for the input impedance,

$$h_{ie} = r_b + (h_{fe} + 1) \frac{m \cdot 26}{i_E},$$

where r_b is the base spreading resistance, i_E is expressed in mA, and m is a factor which, for silicon transistors, lies between 1 and 2.

In general, $i_E = I_E + i_e$.

For Q_3 and Q_4, $I_E = \frac{1}{2} I_{C1}$, and

$$i_e = \tfrac{1}{2} i_{c1}.$$

Similarly, for Q_5 and Q_6, $I_E = \frac{1}{2} I_{C2} = \frac{1}{2} I_{C1}$, and

$$i_e = \tfrac{1}{2} i_{c2} = -\tfrac{1}{2} i_{c1}.$$

Hence, $h_{ie\ 3,4} \equiv h_1 = r_b + (h_{fe} + 1) \dfrac{m \cdot 26}{\frac{1}{2}(I_{C1} + i_{c1})} = r_b + \dfrac{M}{1 + \dfrac{i_{c1}}{I_{C1}}} =$

$$\simeq r_b + \frac{M}{1 + x}, \text{ where } M = \frac{(h_{fe} + 1)\ m \cdot 26}{\frac{1}{2} I_{C1}}, \text{ and } x = \frac{i_{c1}}{I_{C1}}.$$

Similarly, $h_{ie\ 5,6} \equiv h_2 = r_b + (h_{fe} + 1) \dfrac{m \cdot 26}{\frac{1}{2}(I_{C1} - i_{c1})} = r_b + \dfrac{M}{1 - x}$.

Expressing $h_1 - h_2$, $h_1 + h_2$ and $h_1 \cdot h_2$ in terms of r_b, M and x, and substituting these results into equation (2) yields:

$$i_L = h_{fe}\ v_2 \ \frac{-x}{r_b \frac{1 - x^2}{M} (R_2 + r_b) + R_2 + M + 2\ r_b}.$$

For relatively small values of r_b, we may write:

$$i_L = -h_{fe}\ \frac{v_2\ x}{H}, \text{ where } H \simeq R_2 + M.$$

Also, $x = \dfrac{i_{c1}}{I_{C1}} = h_{fe} \dfrac{ib_1}{I_{C1}} = \dfrac{h_{fe}}{I_{C1}} \cdot \dfrac{v_1}{R_1 + 2\ h}$, and hence, the output signal $v_{OUT} = R_L\ i_L$ is given by:

$$\underline{\underline{v_{OUT} = -\frac{h^2_{fe}}{I_{C1}} \cdot \frac{v_1\ v_2}{H\ (R_1 + 2h)}}}.$$